



GREEN, MICROWAVE-ASSISTED SYNTHESIS OF GOLD NANOPARTICLES
USING *CAESALPINIA SAPPAN* HEARTWOOD EXTRACT AND CHITOSAN



A Thesis Submitted in Partial Fulfillment of the Requirements
for Doctor of Philosophy PHARMACEUTICAL SCIENCES (INTERNATIONAL
PROGRAM)

Graduate School, Silpakorn University

Academic Year 2022

Copyright of Silpakorn University



การสังเคราะห์อนุภาคนาโนทองคำแบบเป็นมิตรต่อสิ่งแวดล้อมด้วยคลื่นไมโครเวฟโดย
ใช้สารสกัดจากแก่นฝางและไคโตซาน



วิทยานิพนธ์นี้เป็นส่วนหนึ่งของการศึกษาตามหลักสูตรปรัชญาดุษฎีบัณฑิต
สาขาวิชาวิทยาการทางเภสัชศาสตร์ (หลักสูตรนานาชาติ) แบบ 1.2 ปรัชญาดุษฎีบัณฑิต
บัณฑิตวิทยาลัย มหาวิทยาลัยศิลปากร
ปีการศึกษา 2565
ลิขสิทธิ์ของมหาวิทยาลัยศิลปากร

GREEN, MICROWAVE-ASSISTED SYNTHESIS OF GOLD
NANOPARTICLES USING *CAESALPINIA SAPPAN* HEARTWOOD
EXTRACT AND CHITOSAN



By
MR. Thana THANAYUTSIRI

A Thesis Submitted in Partial Fulfillment of the Requirements
for Doctor of Philosophy PHARMACEUTICAL SCIENCES (INTERNATIONAL
PROGRAM)

Graduate School, Silpakorn University

Academic Year 2022

Copyright of Silpakorn University

Title Green, microwave-assisted synthesis of gold nanoparticles using *Caesalpinia sappan* heartwood extract and chitosan
By MR. Thana THANAYUTSIRI
Field of Study PHARMACEUTICAL SCIENCES (INTERNATIONAL PROGRAM)
Advisor Associate Professor Theerasak Rojanarata, Ph.D.
Co advisor Professor Praneet Opanasopit, Ph.D.
Associate Professor Prasopchai Patrojanasophon, Ph.D.

Graduate School Silpakorn University in Partial Fulfillment of the Requirements for the Doctor of Philosophy

..... Dean of the Pharmacy
(Assistant Professor Surasit Lochidamnuay, Ph.D.)

Approved by

..... Chair person
(Assistant Professor Samarwadee Plianwong, Ph.D.)

..... Advisor
(Associate Professor Theerasak Rojanarata, Ph.D.)

..... Co advisor
(Professor Praneet Opanasopit, Ph.D.)

..... Co advisor
(Associate Professor Prasopchai Patrojanasophon, Ph.D.)

..... Committee
(Associate Professor Malai Satiraphan, Ph.D.)

61356801 : Major PHARMACEUTICAL SCIENCES (INTERNATIONAL PROGRAM)

Keyword : *Caesalpinia sappan*, Gold nanoparticles, Chitosan, Microwave, Extraction
MR. THANA THANAYUTSIRI : GREEN, MICROWAVE-ASSISTED SYNTHESIS OF GOLD NANOPARTICLES USING *CAESALPINIA SAPPAN* HEARTWOOD EXTRACT AND CHITOSAN THESIS ADVISOR : ASSOCIATE PROFESSOR THEERASAK ROJANARATA, Ph.D.

The aims of this work were to develop microwave (MW) assisted synthesis methods for gold nanoparticles (AuNPs) using green reagents as both reducing agents and stabilizing agents and to apply the fabricated products for analytical application. In the first work in which the *Caesalpinia sappan* (CS) heartwood extract was employed, the MW-assisted extraction performed at 300 W for 3 min was used to prepare the extract with high and reproducible brazilin content ($13.1 \pm 0.4\%$ w/w) and it could be readily used for the synthesis of AuNPs. Under the optimal AuNP synthesis conditions i.e. using 5 mL of 1.5 mM HAuCl₄ solution, 0.4 mL of the CS extract and a MW irradiation fixed at 60 °C for 1 min, roughly spherical CS-AuNPs with an average diameter size of 49.6 nm and acceptable 28-day stability were obtained. The resulting CS-AuNPs were capable of selective binding to Fe²⁺, Fe³⁺ and Al³⁺, leading to particle aggregation as well as noticeable change of color and shift of UV-vis absorption maxima at 650 nm. Therefore, they had potential for the colorimetric sensing of certain metal ions in pharmaceutical products. In the second work, chitosan-capped gold nanoparticles (CTS-AuNPs) were synthesized. The synthesis was carried out by using 0.75 mL of 10 mM HAuCl₄ and 5 mL of 0.1% w/v CTS solution and a microwave irradiation at 125 °C for 40 s. The resulting red colloidal solution, showing the maximum absorption peak at 520 nm, contained monodispersed, spherical, and stable CTS-AuNPs with a mean diameter of 17.8 nm. Due to the positively charged surface, CTS-AuNPs were applied to the assay of the polyanionic compound i.e. disodium edetate based on the particle aggregation which eventually induced red-to-blue color change of the solution. It was found that the absorbance at 670 nm related to the disodium edetate concentration with a 4-parameter logistic model. The assay was accurate and precise; its results were comparable to those obtained from the titrimetric pharmacopeial method. Moreover, gold (Au⁰) was shown to be easily recovered from CTS-AuNPs through alkaline-induced precipitation followed by acid treatment and heating, providing a facile and efficient means for treatment of laboratory waste.

ACKNOWLEDGEMENTS

I would like to express my deep appreciation to all those who participated in the creation of this thesis, helped, and supported me throughout my Ph.D. Firstly, I would like to express my sincere thanks to my thesis advisor, Associate Professor Dr. Theerasak Rojanarata, for his invaluable help and constant encouragement throughout the course of this thesis. He gives me the golden opportunity to learn and share, and he builds me up to be a perfect researcher in my own way and always understands me for who I am. I am most grateful for his advice, not only on the research methodologies but also many other methodologies in life. I would not have achieved this far, and this thesis would not have been completed without all the support that I have always received from him. I also would like to express my gratitude to my co-advisor, Professor Dr. Praneet Opanasopit and Associate Professor Dr. Prasopchai Patrojanasophon, for an advice, support, and kindness throughout the course of this research. I would like to thank the Faculty of Pharmacy, Silpakorn University, which is my second home, and staff members for the facilities and other support they provided. Also, I would like to thank all of my friends and the members of the Pharmaceutical Development of Green Innovation Group (PDGIGs) for helping me with all of their power, listening to all my stories, even the good and bad, and trying to build this warm home together. Finally, I most gratefully thank my family for their love, understanding, encouragement, and support throughout the period of this research and throughout my life.

MR. Thana THANAYUTSIRI

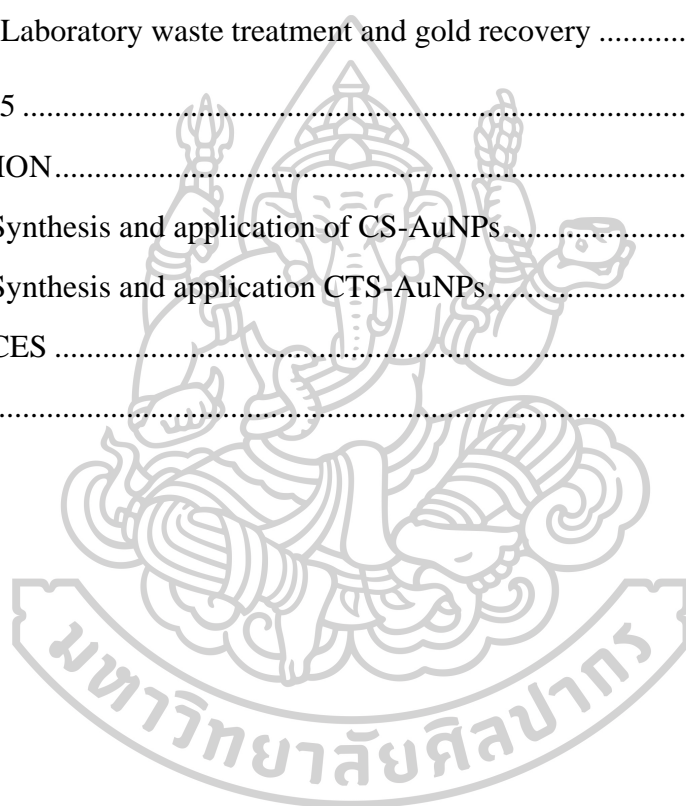
TABLE OF CONTENTS

	Page
ABSTRACT.....	D
ACKNOWLEDGEMENTS.....	E
TABLE OF CONTENTS.....	F
LIST OF TABLES.....	J
LIST OF FIGURES.....	K
LIST OF ABBREVIATIONS.....	1
CHAPTER 1 INTRODUCTION.....	4
1.1 Statement and significance of the research problem.....	4
1.2 Objectives.....	8
1.3 Hypothesis.....	8
CHAPTER 2 LITERATURE REVIEW.....	9
2.1 Gold nanoparticles (AuNPs).....	9
2.1.1 Definition and general characteristics.....	9
2.1.2 Synthesis method of AuNPs.....	10
2.1.3 Application of AuNPs.....	11
2.1.3.1 Drug and gene delivery.....	11
2.1.3.2 Diagnosis sensing.....	11
2.1.3.3 Catalysis.....	12
2.1.3.4 Colorimetric assay.....	12
2.1.4 Recovery of gold from AuNPs.....	12
2.2 Microwave (MW).....	15
2.2.1 Definition.....	15
2.2.2 Advantages and limitations.....	16
2.2.3 MW assisted extraction (MAE).....	17
2.2.4 MW assisted synthesis of AuNPs.....	18

2.3 Brazilin.....	19
2.4 Chitosan (CTS).....	20
CHAPTER 3 MATERIALS AND METHODS	22
3.1 Materials.....	22
3.2 Equipment	23
3.3 Methods.....	24
3.3.1 Development of <i>Caesalpinia sappan</i> capped gold nanoparticles (CS-AuNPs)	24
3.3.1.1 Preparation of CS extract.....	24
3.3.1.1.1 Conventional heating	24
3.3.1.1.2 MW irradiation	24
3.3.1.1.3 Determination of brazilin.....	24
3.3.1.2 Synthesis of CS-AuNPs.....	25
3.3.1.3 Characterizations of CS-AuNPs	25
3.3.1.3.1 Physical appearance.....	25
3.3.1.3.2 Surface plasmon resonance effect	25
3.3.1.3.3 Fourier-transform infrared spectroscopy	25
3.3.1.3.4 Morphology and particle size	26
3.3.1.3.5 Hydrodynamic diameter, size distribution, and zeta potential.....	26
3.3.1.4 Stability study of CS-AuNPs.....	26
3.3.1.5 Preliminary study of metal binding property of CS-AuNPs	26
3.3.2 Chitosan-capped gold nanoparticles (CTS-AuNPs).....	27
3.3.2.1 MW-assisted synthesis of CTS-AuNPs.....	27
3.3.2.2 Characterizations of CTS-AuNPs.....	27
3.3.2.2.1 Physical appearance.....	27
3.3.2.2.2 Surface plasmon resonance effect	27
3.3.2.2.3 Fourier-transform infrared spectroscopy	27
3.3.2.2.4 Morphology and particle size of CTS-AuNPs.....	28

3.3.2.2.5 Hydrodynamic diameter, size distribution, and zeta potential.....	28
3.3.2.3 Development of the colorimetric assay for Na ₂ EDTA injection using CTS-AuNPs	28
3.3.2.3.1 Assay procedure	28
3.3.2.3.2 Method validation.....	28
3.3.2.3.2.1 Linearity and range	28
3.3.2.3.2.2 Limit of detection and limit of quantification	29
3.3.2.3.2.3 Accuracy	29
3.3.2.3.2.4 Intra-day and inter-day precision	29
3.3.2.3.3 Comparison of the proposed method with the standard method.....	29
3.3.2.4 Recovery of gold from laboratory waste and composition analysis	29
3.3.2.5 Statistical analysis	30
CHAPTER 4	31
RESULTS AND DISCUSSION.....	31
4.1 <i>Caesalpinia sappan</i> capped gold nanoparticles (CS-AuNPs).....	31
4.1.1 MW-assisted extraction of CS heartwood.....	31
4.1.2 Optimal condition for MW-assisted synthesis and characteristics of CS-AuNPs	32
4.1.3 Stability of CS-AuNPs	37
4.1.4 Metal ion binding property of CS-AuNPs.....	37
4.2 Chitosan capped gold nanoparticles (CTS-AuNPs).....	39
4.2.1 Optimization of MW-assisted CTS-AuNPs synthesis	39
4.2.2 Characteristics of CTS-AuNPs.....	41
4.2.3 Analytical applicability of CTS-AuNPs	43
4.2.3.1 Principle of the colorimetric assay of edetate disodium.....	43

4.2.3.2 Assay conditions optimization.....	45
4.2.3.2.1 pH of the reaction.....	45
4.2.3.2.2 CTS-AuNPs solution volume.....	46
4.2.3.2.3 Reaction time	46
4.2.3.3 Analytical performance of the assay.....	47
4.2.4 Laboratory waste treatment and gold recovery	51
CHAPTER 5	53
CONCLUSION.....	53
5.1 Synthesis and application of CS-AuNPs.....	53
5.2 Synthesis and application CTS-AuNPs.....	53
REFERENCES	54
VITA.....	64



LIST OF TABLES

Page

Table 1 Regression models representing the relationship of absorbance and concentration of Na ₂ EDTA.....	48
----------------------------------------------------------------------------------------------------------------------	----



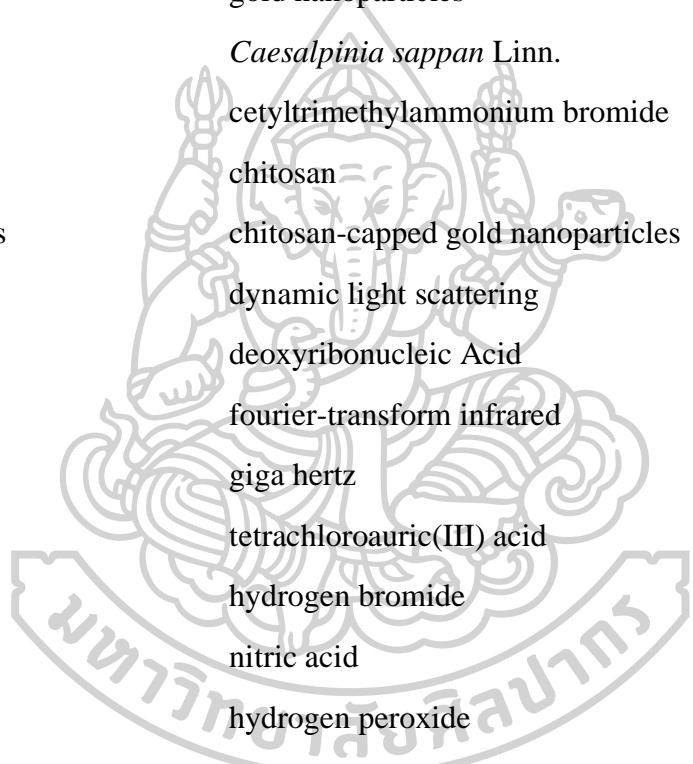
LIST OF FIGURES

	Page
Figure 1 Various shape of the AuNPs [44]	9
Figure 2 Schematic of the gold recovery and recycling process by Pati et al. [66]. ..	13
Figure 3 Images of representative states during gold recovery from nanowaste. From left to right, AuNPs nanowaste waste suspension (A), AuNPs sedimentation by NaCl addition (B), HAuCl ₄ solution after oxidation with HCl + H ₂ O ₂ of gold sediment (C) [67].....	14
Figure 4 The electromagnetic spectrum showing characteristics of MW [69].....	15
Figure 5 The temperature profile after 60 s as affected by MW irradiation (left) compared to treatment in an oil-bath (right) [70].	16
Figure 6 Chemical structure of (a) brazilin and (b) brazilein.	19
Figure 7 Structure of CTS consisting of glucosamine and N-acetyl glucosamine.	21
Figure 8 The amount of brazilin found in the CS extract delivered by (a) the MW-assisted method and (b) conventional heating method using 100°C temperature (n=3).	32
Figure 9 The solution color (shown in circle) and the particle size distribution of CS-AuNPs synthesized with different reactant compositions. Each reaction was performed using the MW-assisted method at the temperature of 60°C for 1 min.....	34
Figure 10 The solution color (shown in circle) and the particle size distribution of CS-AuNPs synthesized with varied time and temperature. Each reaction was performed using the MW-assisted method with 5 mL of 1.5 mM HAuCl ₄ solution and 400 µL of the CS extract as the reactant.	34
Figure 11 (a) The color of the resulting CS-AuNPs colloidal solution and light scattering Tyndall effect and (b) the scanned UV-Vis spectrum of CS-AuNP solution.	35
Figure 12 TEM image of CS-AuNPs.....	35
Figure 13 FTIR spectra of CS-AuNPs (red) and CS extract (blue).	36
Figure 14 The mean of CS-AuNPs hydrodynamic particle size produced using MW irradiation versus conventional heating after 4°C for 28 days storage (n=3). *Signify statistically significant differences.....	37

Figure 15 (a) Color of the CS-AuNPs solutions upon adding metal ions (blank measurement was performed in water), (b) UV-Vis absorption bands shift with added Fe^{2+} , Fe^{3+} or Al^{3+} , and (c) the observed CS-AuNPs agglomeration when Fe^{2+} was added under TEM.	38
Figure 16 UV-Vis spectra of CTS-AuNPs synthesized with varied (a) reaction temperatures (time = 40 s) and (b) time (temperature = 125 °C).	40
Figure 17 Particle size distribution determined by DLS technique of CTS-AuNPs synthesized with various reaction temperatures (rows) and time (column).	41
Figure 18 FTIR spectra of (a) chitosan (red) and (b) CTS-AuNPs (blue).	42
Figure 19 Suggested mechanism of colorimetric reaction occurred among CTS-AuNPs and Na_2EDTA	44
Figure 20 (a) UV-vis spectra of CTS-AuNPs (red) and the CTS-AuNPs interacted with Na_2EDTA (purple), and TEM images of (b) CTS-AuNPs and (c) CTS-AuNPs aggregation.	45
Figure 21 (a) The relationship between the absorbance and pH at a fixed wavelength of 670 nm. The relationship between the absorbance and Na_2EDTA concentration with the effect of (b) pH, (c) CTS-AuNPs volume, and (d) assay reaction time.	47
Figure 22 (a) The image of the colorimetric assay reaction with 0.1–1.2 mM Na_2EDTA and (b) a 4 PL standard curve showing the LOQ of 0.080 mM Na_2EDTA	50
Figure 23 (a) The dried precipitates of CTS-AuNPs (left tube) and citrate-capped AuNPs (right tube) after the treatment with alkaline solution, (b) refined gold solids from CTS-AuNPs wastes, (c) SEM micrograph (top view) of gold grains, and (d) EDS spectrum of gold within the representative microscopic area marked with red-bordered rectangle in (c).	52

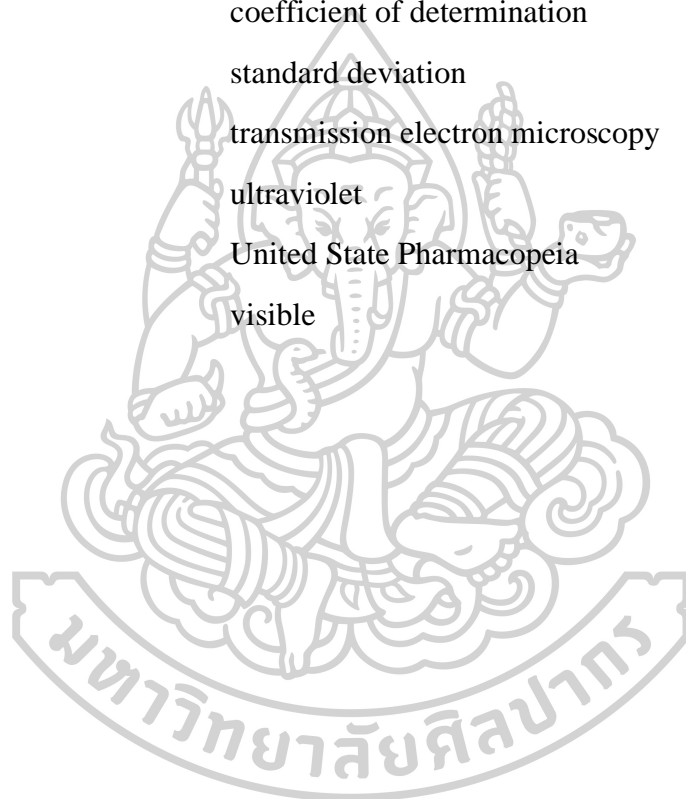
LIST OF ABBREVIATIONS

%	percentage
/	divide
®	registered trademark
±	plus or minus
>	more than
≥	more than or equal
<	less than
≤	less than or equal
°C	degree celsius
et al.	et alia (Latin) means “and others”
i.e.	id est (Latin) means “That is”
e.g.	exempli gratia (Latin) means “for example”
h	hour(s)
min	minute(s)
s	second(s)
L	liter
mL	milliliter
μL	microliter
g	gram
mg	milligram
μg	microgram
M	molar
mM	millimolar
μM	micromolar
N	normality
w/v	weight by volume
v/v	volume by volume



m	meter
cm	centimeter
nm	nanometer
kV	kilovolt
mV	millivolt
W	watt
AuCl ₄ ⁻	tetrachloroaurate ions
AuNPs	gold nanoparticles
CS	<i>Caesalpinia sappan</i> Linn.
CTAB	cetyltrimethylammonium bromide
CTS	chitosan
CTS-AuNPs	chitosan-capped gold nanoparticles
DLS	dynamic light scattering
DNA	deoxyribonucleic Acid
FTIR	fourier-transform infrared
GHz	giga hertz
HAuCl ₄	tetrachloroauric(III) acid
HBr	hydrogen bromide
HNO ₃	nitric acid
H ₂ O ₂	hydrogen peroxide
HPLC	high performance liquid chromatography
ICH	the international council for harmonization
KBr	potassium bromide
LA	labeled amounts
Log	logarithm
LOD	limit of detection
LOQ	limit of quantification
MAE	microwave assisted extraction
MHz	mega hertz

MW	microwave
NaBH ₄	sodium borohydride
Na ₂ EDTA	ethylenediaminetetraacetic acid disodium salt
PDI	polydispersity index
pH	potentia hydrogenii (latin)
4 PL	4-parameter logistic
R.S.D.	relative standard deviation
r ²	coefficient of determination
S.D.	standard deviation
TEM	transmission electron microscopy
UV	ultraviolet
USP	United State Pharmacopeia
Vis	visible



CHAPTER 1

INTRODUCTION

1.1 Statement and significance of the research problem

Gold nanoparticles (AuNPs) are inorganic nanoparticles with particle size range from 1 to 300 nm with a high monodispersity and a large specific surface area. AuNPs are accounted as nontoxic and biocompatible. The use of AuNPs in various disciplines, including chemistry, electronics, engineering, and the biological and pharmaceutical sciences, has been the subject of numerous investigations [1-3]. The development of more effective synthesis methods has also been pursued in an effort to produce gold-based nanomaterials with desired features. Among the different fabrication techniques, environmentally friendly procedures that need nontoxic precursors and moderate reaction conditions, use less energy, and produce less waste have drawn a lot of interest since they are secure, affordable, reasonably quick, and environmentally sustainable. The utilization of reducing and stabilizing agents that are generated naturally from plants [4-6], microbes [7, 8], and biocompatible and renewable substances [9] is one of these greener synthesis techniques. The synthesis of AuNPs has also made use of microwave (MW) irradiation, which is thought to be a more environmentally friendly method of heating. This has sped up the preparation process and saved time, money, and energy [10-12].

Caesalpinia sappan Linn. (CS) or sappan, sappanwood, brazilwood, Indian redwood is a medicinal plant with various application such as a dye for cotton fabric and silk yarn as well as medicinal advantages. The analysis of ethanolic CS extract from heartwood reveals a variety of chemical components, including brazilin and particularly xanthone, coumarin, chalcones, flavones, and homoisoflavonoids. Brazilin is a significant active component found in the heartwood of CS [13, 14]. This organic substance is non-toxic and biocompatible for biomedical use. According to literature, brazilin is a pharmaceutical substance with anti-inflammatory, antibacterial, and antioxidant activities [13, 15-17]. Due to its safety, this natural substance can be developed to be used in food, drinks, cosmetics and textile industries as well as pharmaceutical and medical applications. Brazilin appears as red in an alkaline solution, orange in a neutral solution, and yellow in an acidic solution. Additionally, brazilin is

not stable and is readily oxidized to brazilein due to its higher inclination for degradation [14]. In the chemical structure of brazilin, the carbonyl functional group from oxidation replaces one of the hydroxyl groups in the chemical structure of brazilin, turning the solution to a red color. Also, brazilin could be oxidized to become brazilein when exposed to air and light.

Brazilin from CS is currently rarely used in the synthesis of AuNPs. The only research found to demonstrate the use of CS extract for AuNPs synthesis was by Chartarrayawadee et al. [18] who has effectively used the extract as reducing and stabilizing agents for the environmentally friendly manufacture of AuNPs. Depending on the size of the AuNPs, colloidal solutions of reduced gold ions exhibit natural red-wine and dark purple colors, without interference from the orange/reddish-orange color of the CS extract. For the synthesis and stabilization of AuNPs colloidal solution, effects of CS concentration on the morphology, size, and zeta potential of AuNPs were examined. It was discovered that 0.004-0.04 wt% of CS was the optimal concentration to be used as the reducing agent for green synthesis of AuNPs. Due to the adsorption and stabilizing properties of CS extract, the particle size of AuNPs reduced when CS concentration was raised. The AuNPs were different in size and form with earthworm and quasi-spherical morphologies, according to Transmission electron microscopy (TEM) examination. The stability of AuNPs produced by CS was related to the zeta potential of the obtained particles, which was roughly in the range of -10 mV to -20 mV.

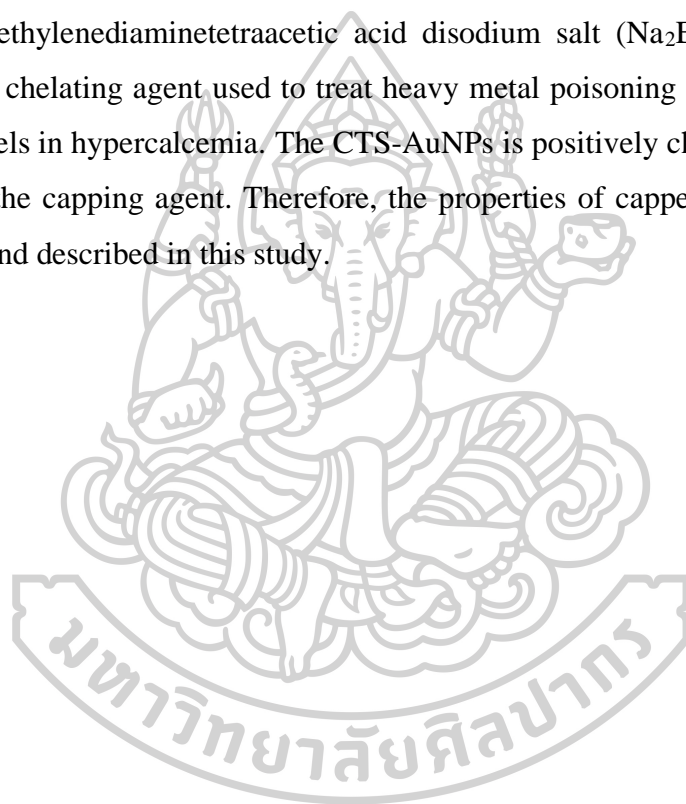
Other than plant extracts, monosaccharides and polysaccharides are well-known naturally abundant biomolecules that have the potential to be effective candidates for the creation of metal nanoparticles due to their reducing and stabilizing properties. Several other kinds of carbohydrates, such as glucose [19], sucrose [20], carrageenan [21], dextran [22], starch [23], agarose [24], gellan gum [25], pectin [26], and fucoidan [27] have been used in the synthesis of AuNPs. Chitosan (CTS) which is made up of N-acetylglucosamine and glucosamine units linked with β -1,4-linkage has also been used in the preparation of stabilized AuNPs that benefited from the aminated moieties. CTS is a green polymer from the standpoint of the environment because it is created naturally and derived from the renewable substance chitin, which is found in the exoskeletons of crustaceans. Additionally, it is biodegradable and harmless. According

to a number of studies, CTS can convert the precursor Au(III) into zero-valent AuNPs by transferring charges from polar functional groups like hydroxyl or amino groups [28]. Additionally, the stabilization and formation of AuNPs are significantly influenced by the electrostatic interactions between the tetrachloroaurate ions (AuCl_4^-) in the solution and the amino groups in CTS; as a result, CTS can function as both a reducing agent and a stabilizing agent for AuNP synthesis [29]. CTS-capped AuNPs (CTS-AuNPs) have recently been created and used for a variety of purposes, including contrast agents for cell and tumor imaging [30], functional nanomaterials for cancer phototherapy [31], carriers for drug and gene delivery [32, 33], and colorimetric sensors [34, 35].

Without the use of other reducing or capping agents, such as sodium citrate or sodium borohydride, the conventional heating method and CTS can be used to synthesize CTS-AuNPs. By heating with the temperature between 70 to 140 °C, the CTS solution and tetrachloroauric acid are mixed with energetic stirring to create the CTS-AuNPs. The appropriate temperature depends on a number of variables, including the concentrations of CTS and gold salt, the ratio of reactants, and the pH of the reaction, which varies among on the studies. Despite the method's simplicity, it takes between 15–120 min [35-40] to synthesize CTS-AuNPs by conventional heating. This considered time- and energy-consuming. MW irradiation is a more effective heating method than the conventional heating because it improves reaction time, product consistency, and requires less energy consumption. Numerous techniques for creating gold nanostructured materials, including AuNPs [41], with the aid of MW have been established recently. Tetrachloroauric acid and CTS solution were combined in a synthesis vessel and irradiated using MW energy, typically using constant power (watt) set at the proper level [42, 43], in various experiments on the synthesis of CTS-AuNPs. The outcomes of these investigations showed that the time required for the synthesis was reduced drastically to 1-3 min.

Until now, the use of AuNPs in analytical chemistry and quality control has not yet met its capability. Thus, this study aimed to utilize AuNPs for quantitative analysis of different compounds using AuNPs synthesized with MW-assisted method. The purpose of this work was to investigate the MW-assisted synthesis of AuNPs with the presence of CS extract. Brazilein, an oxidized compound from CS extract, was known

to be able to interact with specific metals; the capacity of brazilein-capped AuNPs to interact with metals and cause aggregation leading to color change was examined. Moreover, CTS-AuNPs preparation using MW-assisted synthesis in a fixed temperature mode, referring to the MW source itself regulates the power sent to the reactor to keep the temperature consistent throughout the synthesis has not yet been reported. The optimal condition for the synthesis of CTS-AuNPs was studied to provide a new avenue for the synthesis as an alternative procedure. The CTS-AuNPs were then used as a colorimetric sensor for the quantitative determination of the anionic compound ethylenediaminetetraacetic acid disodium salt (Na_2EDTA), which is an intravenous chelating agent used to treat heavy metal poisoning and lower the serum calcium levels in hypercalcemia. The CTS-AuNPs is positively charged due to the use of CTS as the capping agent. Therefore, the properties of capped AuNPs have been illustrated and described in this study.



1.2 Objectives

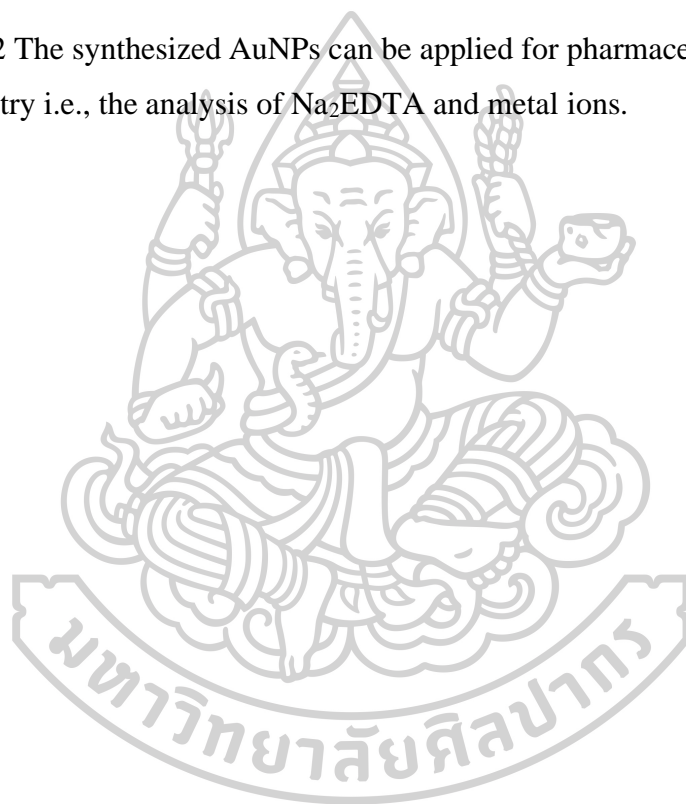
1.2.1 To develop green and rapid MW-assisted synthesis of AuNPs using the CS heartwood extract and CTS.

1.2.2 To apply the AuNPs synthesized by using CS extract and CTS for the pharmaceutical analysis i.e., sensing of metal ions and assay of Na₂EDTA, respectively.

1.3 Hypothesis

1.3.1 AuNPs can be synthesized by green and rapid method using CTS and the heartwood extract of CS with the aid of MW irradiation.

1.3.2 The synthesized AuNPs can be applied for pharmaceutical analysis based on colorimetry i.e., the analysis of Na₂EDTA and metal ions.



CHAPTER 2

LITERATURE REVIEW

2.1 Gold nanoparticles (AuNPs)

2.1.1 Definition and general characteristics

AuNPs are tiny particles of gold (Au^0) that have diameters in the nanoscale, typically ranging from 1 to 100 nm. AuNPs have colors depending on size, shape and distance between them. For small (~30 nm) monodisperse AuNPs, the surface plasmon resonance phenomenon causes an absorption of light in the blue-green portion of the spectrum (~450 nm) while red light (~700 nm) is reflected, yielding a rich red color. As particle size increases, the wavelength of surface plasmon resonance related absorption shifts to longer, redder wavelengths. Red light is then absorbed, and blue light is reflected, yielding solutions with a pale blue or purple color.

AuNPs have unique optical, electronic, and chemical properties that are different from bulk gold, making them useful in a variety of applications such as catalysis, drug delivery, and sensing. They can be synthesized in various shapes, sizes, and surface chemistries, and can be functionalized with a variety of ligands or other chemical groups to tune their properties. By different synthesis method used and the reaction conditions, AuNPs obtained can have a variety of shapes, including spheres, rods, cubes, and more complex shapes such as triangles, hexagons, and stars (Figure 1).



Figure 1 Various shape of the AuNPs [44]

2.1.2 Synthesis method of AuNPs

There are several methods for synthesizing AuNPs, including physical, chemical, and biological methods.

- **Physical methods** involve the use of physical forces to reduce gold ions AuNPs. One common method is laser ablation [45].
- **Chemical methods** involve the use of chemical reduction agents to reduce gold ions to AuNPs. The most common methods rely on the use of citrate or sodium borohydride (NaBH₄) as reducing agent. conventional methods used for AuNPs synthesis is Turkevitch method in 1951. Turkevitch used citrate solution as reducing agent to reduce gold (III) derivatives, namely HAuCl₄ to gold with zero valency [46]. Later, the use of had been developed to eliminate the heating process.

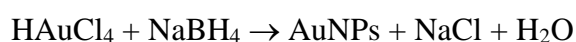
- Turkevitch method

The Turkevitch method was developed in 1951 [47], and it is then a widely used method for synthesizing AuNPs. It involves the reduction of gold ions by sodium citrate with the aid of heat. Citrate ion also act as a capping or stabilizing agent to prevent the aggregation of nanoparticles. In some circumstance, additional stabilizing agent, such as cetyltrimethylammonium bromide (CTAB), polyethylene glycol (PEG), polyvinylpyrrolidone (PVP), is added to enhance the product stability.



- Sodium borohydride (NaBH₄) method

NaBH₄ is a strong reducing agent that is highly reactive with gold ions, leading to rapid reduction and formation of the nanoparticles. By this method, heating is unnecessary.



- **Biological methods** involve the use of microorganisms or enzymes to synthesize AuNPs [48]. Example of a biological method are the use of bacteria [49] or fungi [50] to produce AuNPs, which can be achieved by reducing gold ions with the microbial metabolic byproducts. In addition, AuNPs can be synthesized by the use of plant extracts which contain various biomolecules

such as flavonoids [51], terpenoids [52] and polyphenols [53] acting as a reducing agent and stabilizing agent.

2.1.3 Application of AuNPs

2.1.3.1 Drug and gene delivery

The advantages of AuNPs are their high stability and biocompatibility, which make them suitable for use in the human body. AuNPs can be easily functionalized with a variety of biomolecules, such as proteins, nucleic acids, and small molecules, which allows them to be targeted to specific cells or tissues in the body.

In drug delivery, AuNPs can be used to deliver therapeutic agents directly to the site of disease, which can improve the effectiveness of treatment and reduce side effects. AuNPs can also be used to deliver gene therapies, which involve the introduction of functional genetic material into cells to treat or prevent disease. Examples of the use of AuNPs for drug and gene delivery are;

- Doxorubicin loaded gold nanoparticles to use as passive targeting on anticancer efficacy [54].
- Gold nanoparticles loaded with docetaxel [55].
- Polymer functionalized gold nanoparticles as nonviral gene delivery reagents [56].

2.1.3.2 Diagnosis sensing

AuNPs have also been used in the development of diagnostic sensing technologies for detecting a variety of diseases and conditions [57]. For example, AuNPs functionalized with specific antibodies or other biomolecules have been used to detect cancer markers in blood or tissue samples, to detect infectious diseases such as HIV or tuberculosis, and to diagnose a range of other conditions such as diabetes or cardiovascular disease. Examples of the use of AuNPs for diagnostic sensing are;

- Electrochemiluminescence of gold nanoparticles and gold nanoparticle-labelled antibodies as co-reactants [58].
- Fluorescence near gold nanoparticles for DNA sensing [59].
- Generation of cytotoxic singlet oxygen via phthalocyanine-stabilized gold nanoparticles: a potential delivery vehicle for photodynamic therapy [60].

2.1.3.3 Catalysis

The important properties of AuNPs that suitable for catalysts is their high surface area, which allows them to interact with a large number of reactant molecules simultaneously. This can increase the efficiency of the catalytic process and result in higher yields of the desired product. Examples of the use of AuNPs for catalytic are;

- Supported gold nanoparticles as catalysts for the oxidation of alcohols and alkanes [61].
- Gold nanoparticle catalysts for selective hydrogenations [62].

2.1.3.4 Colorimetric assay

AuNPs have been widely used in colorimetric assays, which are analytical techniques that measure the concentration of a substance by measuring the color of a solution.

In a colorimetric assay using AuNPs, the substance of interest interacts with the AuNPs solution, inducing the aggregation of nanoparticles. This phenomenon leads to the change their color due to the alteration of the size and shape of the particles.

The change in color can be measured using a spectrophotometer, which measures the intensity or wavelength of the light absorbed or transmitted by the solution. By comparing the color of the solution before and after the substance is added, it is possible to determine the concentration of the substance in the sample. Examples of the use of AuNPs for colorimetric assay are;

- A simple and sensitive colorimetric assay for determining mercury(II) ion using gold nanoparticles [63].
- A colorimetric assay for D-Penicillamine in urine and plasma samples based on the aggregation of gold nanoparticles [64].
- Colorimetric assay using gold nanoparticles for trace determination of tolyltriazole in aqueous media [65].

2.1.4 Recovery of gold from AuNPs

The production and use of AuNPs result in consequent generation of nanowaste. Since Au(III) salts, a precursor of AuNPs are expensive resources, some attempts have been made to develop a methodology which allows laboratory scale gold recovery and/or its transformation into new AuNPs. In addition, the recovery and recycling of

these materials is important nowadays because of the environmental issues in terms the management of sustainable materials when non-renewable resources are involved. Moreover, the potential risks of nanomaterials and their impact to human beings and the environment are currently insufficiently understood and could become a key point in the future.

From the literature review, the Pati et al. [66] reported focused on AuNPs capped with citrate recovery and recycling (Figure 2). In this work, β -cyclodextrin was used for Au(III) extraction after oxidation, employing a mixture $\text{HBr} : \text{HNO}_3 = 3 : 1$, of a simulated aqueous nanowaste containing AuNPs. Afterwards, several steps of reduction, precipitation and oxidation were carried out, allowing to obtain a gold solution that was employed to synthesis of AuNPs. However, the obtained AuNPs, which contained unidentified impurities, were unstable and coalesced.

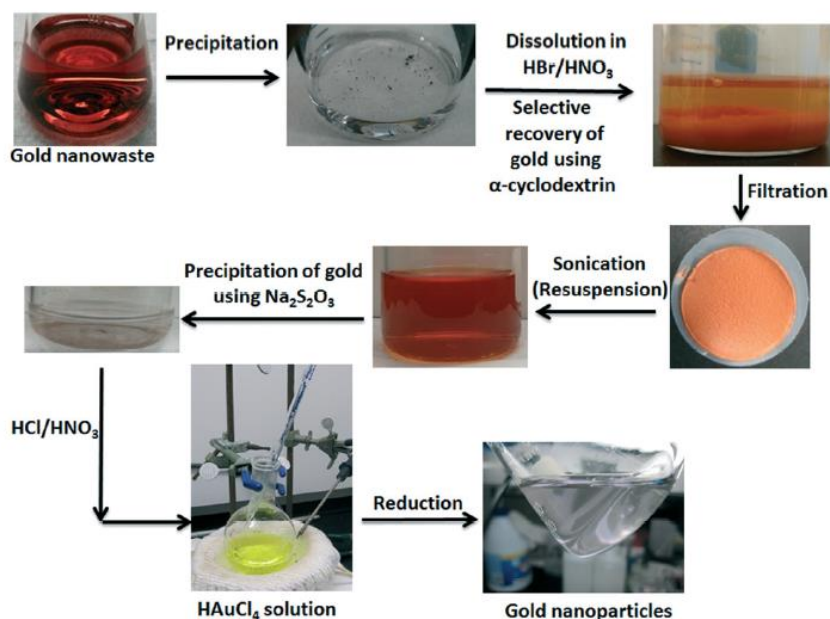


Figure 2 Schematic of the gold recovery and recycling process by Pati et al. [66].

In another work [67], Au(III) was recovered from aqueous laboratory nanowaste, using commonly available reagents (Figure 3). The recovery process involves three-steps: (1) AuNPs separation from real or simulated nanowaste by salting-out; (2) aqueous HAuCl_4 solution preparation employing a mixture of hydrogen

peroxide and hydrochloric acid.; (3) Au nanospheres synthesis employing a seeded growth approach. This process allowed the recovery of more than 99% of the original gold.

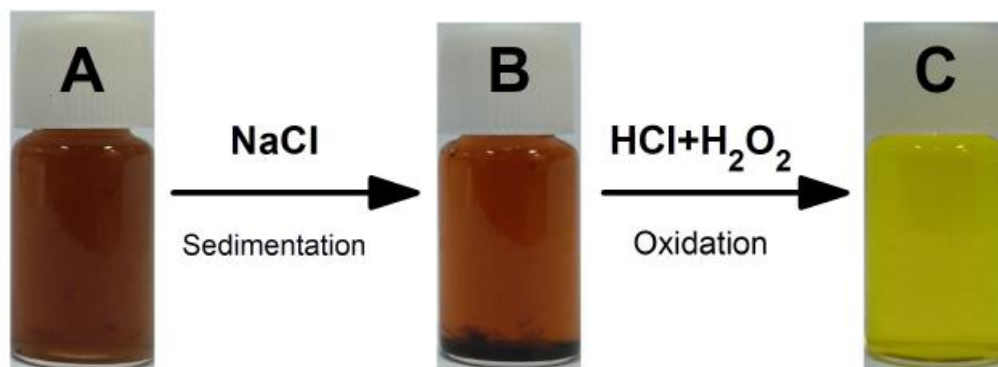
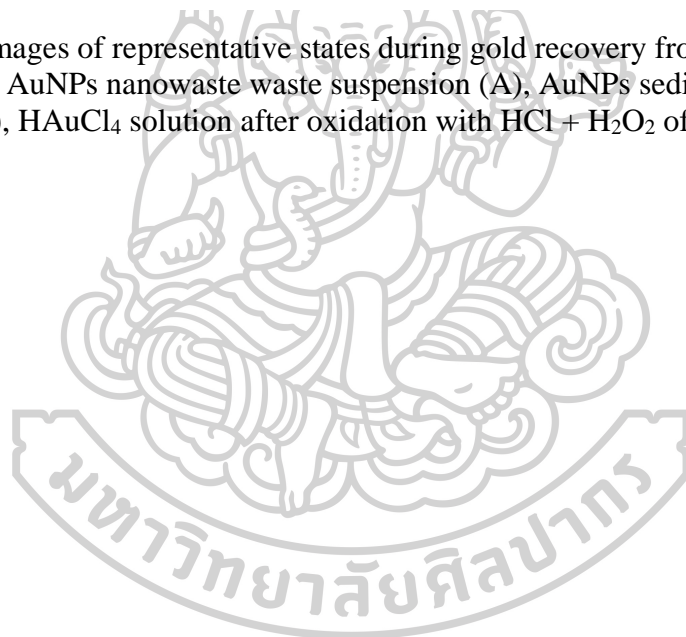


Figure 3 Images of representative states during gold recovery from nanowaste. From left to right, AuNPs nanowaste waste suspension (A), AuNPs sedimentation by NaCl addition (B), HAuCl₄ solution after oxidation with HCl + H₂O₂ of gold sediment (C) [67].



2.2 Microwave (MW)

2.2.1 Definition

MW are electromagnetic radiations with wavelengths ranging from about 1 m to 1 mm. and frequencies between 0.3 and 300GHz (Figure 4). MW are commonly used in telecommunications, radar, and MW ovens. Most commercial MW ovens are designed for operation at 2450 MHz [68]. In a laboratory setting, a MW is a device that uses to produce quickly and uniformly heat the sample or reactants, which can facilitate the extraction or synthesis process.

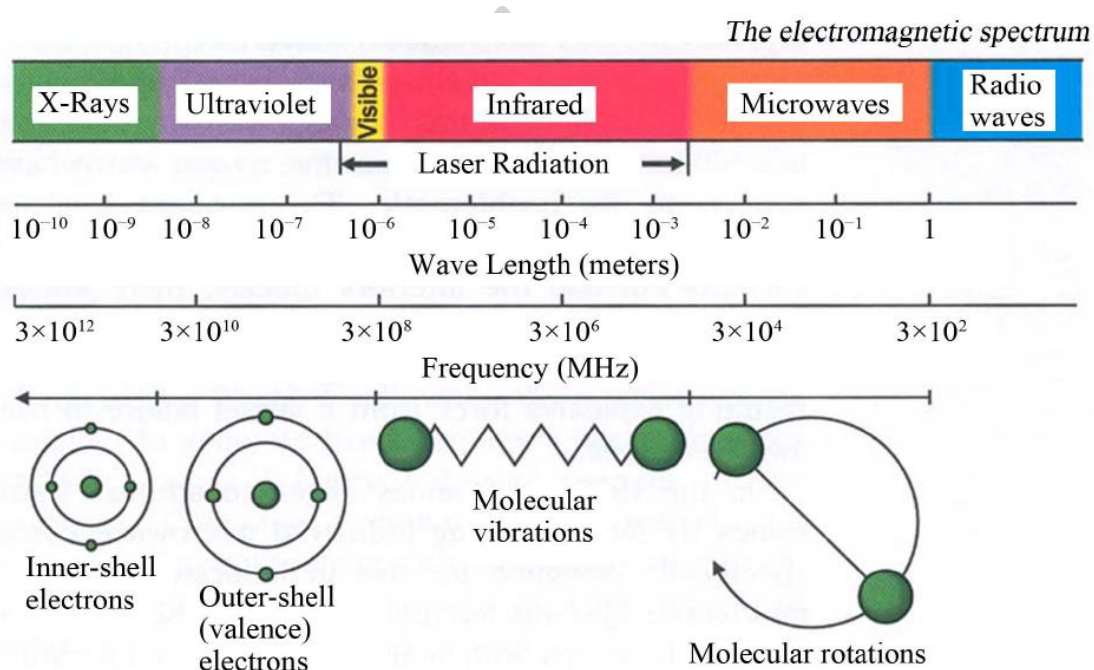


Figure 4 The electromagnetic spectrum showing characteristics of MW [69].

MW irradiation produces heat by causing the water molecules in the sample to rotate by two main mechanisms: dipolar polarization and ionic conduction. This vibration produces heat, which is then transferred to the rest of the sample. The heat generated by the MW can help to dissolve or extract the desired compounds from the sample, making them more readily available for analysis or further processing.

Different from a conventional heating method that the vessel surface is contacted with the heat source, the heat of reaction mixture caused by MW proceeds directly inside the material avoiding the reaction vessel (Figure 5). This means that the reaction proceeds rapidly and uniformly in the reaction vessel. In addition, the

temperature of a MW irradiated substrate can be raised higher than its boiling point, i.e., superheating, but the highest temperature of conventional heating is limited by boiling point of a substrate. Furthermore, MW irradiation provide the synthesis reaction with MW effects, i.e., those resulting from the material and wave interactions and the dipolar polarization, in addition to the effects of efficient heating

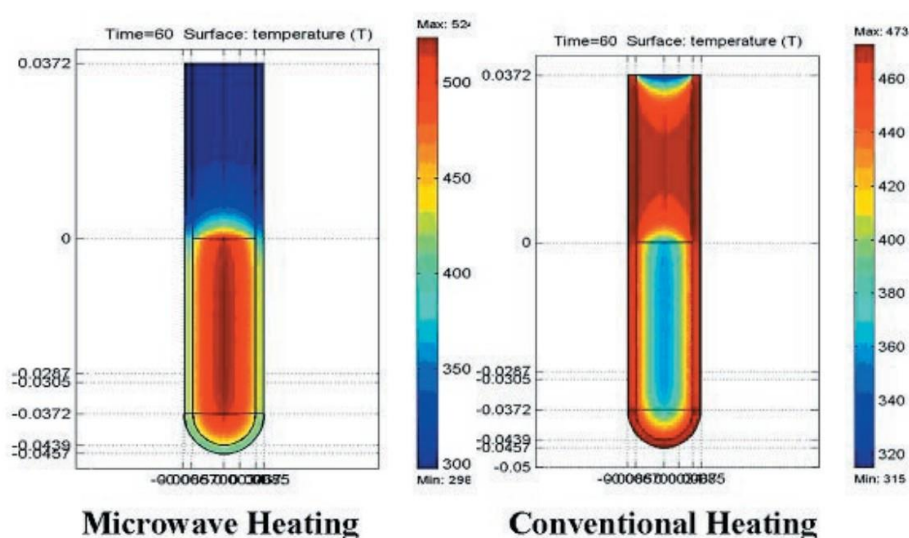


Figure 5 The temperature profile after 60 s as affected by MW irradiation (left) compared to treatment in an oil-bath (right) [70].

2.2.2 Advantages and limitations

The advantages and limitation of MW that have been discussed in many literatures [68, 71-75] which are summarized below

Advantages:

- **Speed:** MW can heat and dry samples much faster than conventional methods, such as heating on a hot plate. This can save time and increase productivity in the laboratory.
- **Efficiency:** MW are more energy-efficient than conventional heating methods because they directly heat the sample rather than heating on the vessel surface surrounding the sample. In addition, the temperature of a substrate can be raised higher than its boiling point, i.e., superheating may take place. This can result in energy savings and reduced operating costs.

- Uniform heating: MW can uniformly heat the sample, which can be beneficial for certain types of reactions or processes that require uniform heating.
- Controllability: MW can be precisely controlled and adjusted, which allows for precise temperature control and the ability to monitor the heating process.

Limitations:

- Compatibility: Not all materials are suitable for MW heating or synthesis. Some materials, such as metals and certain types of glass, can reflect MW and may not be heated efficiently.
- Safety: Care must be taken when using MW in the laboratory to ensure the safety of the operator. MW ovens must be properly grounded and shielded to prevent leaks, and proper safety precautions must be followed to prevent burns or other injuries.
- Cost: MW equipment can be more expensive than conventional heating equipment.
- Limited application: MW may not be suitable for all types of heating or synthesis processes. For example, they may not be suitable for processes that require very high temperatures or for certain types of reactions that are sensitive to MW.

2.2.3 MW assisted extraction (MAE)

Extraction is a common and essential step in many analytical chemistry techniques. MAE is a recent extraction technique available to analysts. It involves the use of MW to facilitate the extraction process, and it offers several advantages over traditional extraction methods. One of the main benefits of MAE is the ability to perform extractions more rapidly and efficiently, which can lead to significant time savings and cost reductions. In addition, MAE can often provide more complete and reproducible extractions, as it can effectively extract a wider range of analytes from various sample matrices. In MAE, MW are used to generate heat and pressure within a MW-transparent solvent, which can then be used to extract analytes from the sample matrix. There are several factors that can influence the efficiency of MAE, including the temperature and pressure of the solvent, the type and concentration of the solvent,

and the duration of the extraction. they can significantly impact the quality and reproducibility of the resulting extract.

In many studies, it has been reported that MW irradiation causes disruption of plant cells, thereby facilitating the mass transfer of solvent into the plant material and the release of the plant constituents [76]. Therefore, it is more efficient extraction method than conventional heating in terms of the requirement of less solvent and energy consumption, higher yield and faster operation [77].

Example of MAE are described in several articles e.g. Chan et al.(2011) [77], Llompart et al.(2019) [78], Mirzadeh et al.(2020) [79].

2.2.4 MW assisted synthesis of AuNPs

For the synthesis of AuNPs, MW irradiation has potential to significantly reduce the synthesis time and improve the yield. In addition, it is more energy-efficient and safer. In term the characteristics of the products, it is usually found that MW produce smaller size, narrow uniformity and higher stability compared to conventional methods [70]. Example of MW assisted synthesis of AuNPs are;

- Nguyen et al. [80] compared MW-assisted synthesis of AuNPs using *Ganoderma lucidum* extract with the conventional method. The result showed that MW irradiation at 400 W only for 10 min could produce AuNPs whereas conventional used 6 h at 85 °C. In addition, the particle size, yield and size distribution of AuNPs obtained from MW method were better than those prepared by conventional method.
- Arshi et al. [81] produced AuNPs by mixing HAuCl₄, citric acid and CTAB then irradiated by MW at 100 W for 40 s. The resulted AuNPs had a diameter range of 1-10 nm and showed high antibacterial activity against *E. coli* (ATCC 25922 strain).
- Sunkari et al. [82] used Papaya leaf extract to reduce the HAuCl₄ by MW assisted synthesis. The AuNPs could be produced at 750 W for 90 s. The AuNPs had the average size of 15 ± 2 nm. The papaya leaf extract capped AuNPs showed effective antibacterial activity on both *P. putida* and *S. aureus*.

2.3 Brazilin

Brazilin, (6a*S*-cis) (7,11b-dihydrobenz[*b*]indeno[1,2-*d*]pyran-3,6a,9,10,(6*H*)-tetr_{ol}) (Figure 6(a)), is a red colored, water soluble homoisoflavonoid. It is a main constituent found in the heartwood of CS, a plant in the family of Caesalpiniaceae which is widely distributed in Southeast Asia. Brazilin can be oxidized, by exposure to atmospheric oxygen and light, to brazilein or 6a*S*-(6a,7-dihydro-3,6a,10-trihydroxybenz[*b*] indeno[1,2-*d*]pyran-9(6*H*)-one) (Figure 6(b)). Traditionally, the aqueous extracts from the wood of CS are used for the dyeing of fabrics [83]. In addition, scientific studies of CS have reported various pharmacological effects of brazilin and CS heartwood extract, including antioxidant activity, antibacterial activity, antiacne activity, anti-inflammatory activity, hypoglycemic activity, hepatoprotective activity and vasorelaxation activity [13, 83].

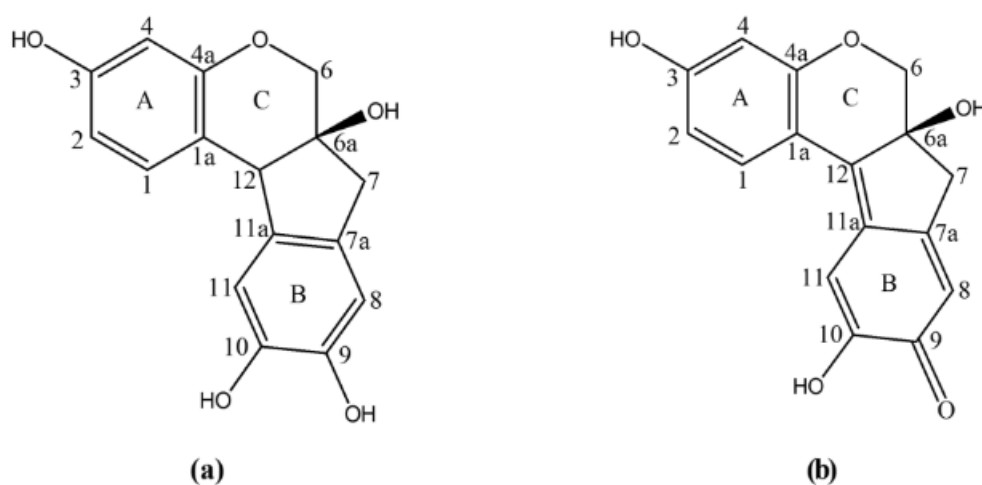


Figure 6 Chemical structure of (a) brazilin and (b) brazilein.

To obtain brazilin or red dye from sappan wood, a traditional method is based on boiling of wood pieces in water. Also, Chartarrayawadee et al. [18] prepared the CS extract in water by conventional heating at 80°C for 3 h for the synthesis of AuNPs. In laboratory, extractions of CS heartwood are usually carried out by using mainly organic solvents e.g. ethanol, methanol and the mixture of alcohol and water as solvents [84,

85]. In addition, the MAE [86, 87] and the subcritical solvent extraction [88] were reported.

Since CS extract which contains brazilin and other phytochemicals such as polyphenols and flavonoids can act as a reducing agent, its applicability for the synthesis of AuNPs has been investigated. However, the study is currently limited. Until now there is the only work carried out by Chartarrayawadee et al. [18] In that work, the solution of lyophilized CS extract was mixed with HAuCl_4 solution. Subsequently, the mixture was stirred overnight (12 h) at room temperature followed by heating the solution at 90°C for 1 h, resulting in quasi-spherical and short-length earthworm-like shaped CS-AuNPs with the average hydrodynamic size of 49 nm [10].

Since brazilin can form the complex by coordinate covalent bonds with selectivity to certain metal ions such as Al^{3+} [89] and Fe^{2+} , it was also used for colorimetric detection of Fe^{2+} via a ratiometric absorption response to Fe^{2+} at 539 nm and 615 nm [90]. However, until now there is no report about the possibility of using brazilin or brazilein which is caps on the AuNPs for the analysis of metal ions.

2.4 Chitosan (CTS)

CTS is a biodegradable, biocompatible, and non-toxic macromolecule. It consists of glucosamine and N-acetyl glucosamine units linked together by β -1,4-glucosidic bonds (Figure 7) [91]. CTS has a molecular weight ranging from a few hundred to several hundred thousand daltons, depending on the degree of deacetylation and the method of synthesis. It is insoluble in water, but soluble in dilute acidic pH (pH 2-6). As the degree of deacetylation increases, the solubility increases. CTS is a polycationic polymer with a pKa on amine group around at 6.17 to 6.51 [92]. It is produced from degradation of chitin on the shell of marine crustaceans such as shrimp and crab induced by certain groups of bacteria that produce the enzymes deacetylase or chitosanase enzymes. In medical and pharmaceutical fields, CTS can be used for several applications such as tissue engineering [93, 94], wound healing [95, 96], drug delivery [97, 98], medication [99, 100] and gene therapy [101].

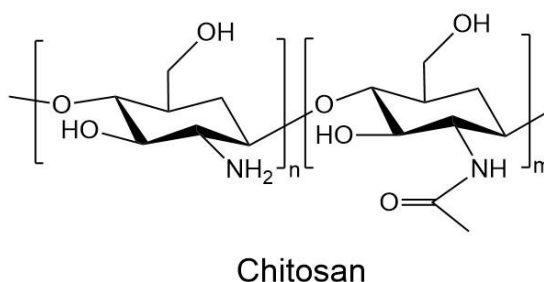


Figure 7 Structure of CTS consisting of glucosamine and N-acetyl glucosamine.

CTS-AuNPs can be synthesized by conventional synthesis methods using sodium citrate or NaBH_4 as a reducing agent and then adding CTS as a capping agent. For example, Chen et al. [34] prepared CTS-AuNPs by reducing HAuCl_4 solution with trisodium citrate. Then, CTS was added. The resulting CTS-AuNPs could be used for colorimetric sensing of heparin. Bhattarai et al. [102] used NaBH_4 to reduce HAuCl_4 in the presence of CTS at room temperature. The resulting AuNPs could immobilize nicked plasmid DNA to enhance DNA delivery.

Apart from the conventional synthesis method which uses toxic reducing agents, CTS can be used for that purpose as both a reducing agent and capping agent by itself. In 2017, 0.1% (w/v) CTS was mixed with HAuCl_4 with heating for 45 min. The AuNPs solution showed red color with the particle size of AuNPs in the range of 24 - 30 nm in diameter [103]. These CTS-AuNPs could be used for the detection of amplified nucleic acids isolated from sputum. In addition, the MW-assisted synthesis of CTS-AuNPs had been developed. This method reduced the synthesis reaction time to 40 - 60 s [41, 43].

CHAPTER 3

MATERIALS AND METHODS

3.1 Materials

1. Aluminum sulfate octadecahydrate ($\text{Al}_2(\text{SO}_4)_3 \cdot 18\text{H}_2\text{O}$) (Sigma-Aldrich®, St. Louis, MO, USA)
2. Boric acid ($\geq 99.5\%$) (Sigma-Aldrich®, St. Louis, MO, USA)
3. Brazilin standard ($\geq 99.0\%$) (Chengdu Biopurify Phytochemical Ltd., China)
4. *Caesalpinia sappan* Linn. Powder
5. Calcium sulfate dihydrate ($\text{CaSO}_4 \cdot 2\text{H}_2\text{O}$) (Sigma-Aldrich®, St. Louis, MO, USA)
6. Chitosan (low molecular weight, 50-190 kDa, 75%–85% degree of deacetylation) (Sigma-Aldrich®, St. Louis, MO, USA)
7. Disodium edetate (Na_2EDTA) dihydrate ($\geq 99.0\%$) (Sigma-Aldrich®, St. Louis, MO, USA)
8. Ferric chloride hexahydrate ($\text{Fe}(\text{III})\text{Cl}_3 \cdot 6\text{H}_2\text{O}$) (Sigma-Aldrich®, St. Louis, MO, USA)
9. Ferrous sulfate heptahydrate ($\text{Fe}(\text{II})\text{SO}_4 \cdot 7\text{H}_2\text{O}$) (Sigma-Aldrich®, St. Louis, MO, USA)
10. Glacial Acetic Acid (Merck, Germany)
11. Gold (III) chloride trihydrate ($\text{HAuCl}_4 \cdot 3\text{H}_2\text{O}$) ($\geq 99.0\%$) (Sigma-Aldrich®, St. Louis, MO, USA)
12. Hydrochloric acid fuming, $\geq 37\%$ (Merck, Germany)
13. Magnesium sulfate heptahydrate ($\text{MgSO}_4 \cdot 7\text{H}_2\text{O}$) (Sigma-Aldrich®, St. Louis, MO, USA)
14. Methanol (Merck, Germany)
15. Na_2EDTA dihydrate injection
16. Nitric Acid (Merck, Germany)
17. Phosphoric acid (≥ 85 wt. % in H_2O) (Merck, Germany)
18. Potassium bromide (KBr) (FT-IR grade, $\geq 99\%$) (Sigma-Aldrich®, St. Louis, MO, USA)
19. Potassium sulfate (K_2SO_4) (Sigma-Aldrich®, St. Louis, MO, USA)

20. Sodium hydroxide ($\geq 97.0\%$, pellets) (Sigma-Aldrich®, St. Louis, MO, USA)
21. Sulfuric acid (95.0-98.0%) (Merck, Germany)
22. Zinc sulfate heptahydrate ($\text{ZnSO}_4 \cdot 7\text{H}_2\text{O}$) (Sigma-Aldrich®, St. Louis, MO, USA)

3.2 Equipment

1. Analytical balance (Sartorius AG Gottingen, Germany)
2. C18 HPLC column (4.6 x 150 mm, 4.6×150 mm, 5 μm ; Cosmosil® Japan)
3. High Performance Liquid Chromatography (HPLC) (Agilent 1260 Series, Agilent Technologies, Santa Clara, CA, USA)
4. LCD Digital Magnetic Hotplate Stirrer MS-H380-Pro (Onilab LLC, USA)
5. Microcentrifuge (Microfuge® 16 Centrifuge, Beckman Coulter)
6. Micropipette (Eppendorf Research®, Eppendorf, Germany)
7. Microplate reader (Victor Nivo™ Multimode plate reader, Perkin Elmer, UK)
8. Microwave (MW) synthesizer (Discover SP, CEM Corporation, USA)
9. pH meter (LAQUAtwin pH, HORIBA, Japan)
10. Scanning electron microscopy (SEM, Tescan Mira3) coupled with energy-dispersive X-ray spectroscopy (EDS, Element EDS System, EDAX)
11. Thermo Nicolet Nexus 4700 FTIR spectrometer (Thermo Fisher Scientific, USA)
12. Transmission electron microscopy (TEM, Philips® Model TECNAI 20, OR, USA)
13. UV/Visible spectrophotometer (Cary 60 UV-Vis, Agilent Technologies, Santa Clara, CA, USA)
14. Vortex mixer (VX100, Labnet International Inc., USA)
15. Zetasizer Nano ZS (Malvern Instruments, UK)

3.3 Methods

3.3.1 Development of *Caesalpinia sappan* capped gold nanoparticles (CS-AuNPs)

3.3.1.1 Preparation of CS extract

3.3.1.1.1 Conventional heating

One gram of CS heartwood powder was accurately weighed in a 50-mL glass vessel, then 20 mL of water was added. The vessel was placed to boil in a 100 °C water bath with vigorous stirring. At different timepoints (5, 15, 30, 60 min), 1 mL of the extract was withdrawn from the vessel, centrifuged, and filtered to obtain a clear solution. The solutions were kept in a refrigerator at 4 °C until further use.

3.3.1.1.2 MW irradiation

A dispersion of CS heartwood powder was prepared in a 50-mL glass vessel (1 g in 20 mL of water). Then, the glass vessel was placed in a MW synthesizer (Discover SP, CEM Corporation, USA) and irradiated using 100, 200, or 300 W power with a fixed power mode. The reaction time was varied to be 1, 2, and 3 min. Subsequent to the reaction completion, the vessel was removed from the reactor, and the clear solution was kept at 4 °C after centrifugation and filtration.

3.3.1.1.3 Determination of brazilin

The brazilin content in the extracts was quantified using HPLC analysis (Agilent 1260 Infinity, Agilent Technologies, USA) following the method reported by Warinhomhaun et al. [84] A C18 column (4.6 × 150 mm, 5 μm) was used as a stationary phase, while the mobile phase was a gradient flow of solution A (methanol) and solution B (methanol:2.5% acetic acid (10:90)). The flow started with the ratio of solution A:B at 10:90 for 12 min and shifted to 100% of solution A and hold for 13 min. Thereafter, the mobile phase was altered back to the initial ratio and maintained for 15 min. The injection volume, flow rate, detection wavelength, and column temperature were 20 μL, 1.0 mL/min, 280 nm, and 35°C, respectively. The retention time of brazilin was 10.2 min. The extraction condition that yields the highest content of brazilin was selected for the following experiments.

3.3.1.2 Synthesis of CS-AuNPs

The reduction reaction was used to prepare CS-AuNPs in which the CS extract was employed as the reducing agent and stabilizing agent. A HAuCl_4 solution was reduced in a MW synthesizer using dynamic control mode. Several parameters composing of HAuCl_4 concentration, volume of CS extract, reaction time, and temperature was varied to optimize the synthesis procedure. Precisely, the substrate concentration was varied by 0.5, 1.0, and 1.5 mM with the final volume maintained at 5 mL. The CS extract volume was 200, 400, and 600 μL . The reaction time was 0.5, 1, 2 min, while the temperature was varied at 50, 60, and 70 $^\circ\text{C}$. Immediately after the reaction by MW irradiation, the gold colloid solutions were cooled in an ice bath. The resulting CS-AuNPs were stored in a refrigerator until use.

3.3.1.3 Characterizations of CS-AuNPs

3.3.1.3.1 Physical appearance

The physical characteristics considering color and clarity of the colloidal CS-AuNPs were investigated visually. Tyndall effect was used to examine the colloidal property where a laser beam is given to the sample solution and light scattering phenomenon of the colloidal systems is observed.

3.3.1.3.2 Surface plasmon resonance effect

AuNPs possess surface plasmon resonance effect which can be determined by the ultraviolet-visible (UV-Vis) spectrophotometer. The bands of CS-AuNPs were scanned and collected in the wavelength range of 400-800 nm using a multimode plate reader (Victor Nivo, PerkinElmer, USA).

3.3.1.3.3 Fourier-transform infrared spectroscopy

The chemical attribute of CS-AuNPs were analyzed using Fourier-transformed infrared (FTIR) spectroscopy (Thermo Nicolet Nexus 4700 FTIR spectrometer, Thermo Fisher Scientific, USA). The samples were obtained after centrifugation of the AuNPs solutions at 14,000 rpm for 15 min. Then, the supernatant was removed and the solid particles were washed with water and leave to dry in a hot air oven at 70 $^\circ\text{C}$ overnight. Also, the AuNPs colloidal samples were dried using lyophilization technique. The dried AuNPs were acquired in the KBr disc preparation for the

measurement in the spectrophotometer to compare the spectra of AuNPs dried using different technique.

3.3.1.3.4 Morphology and particle size

The morphology of CS-AuNPs as well as the particle size was observed under a transmission electron microscope (TEM, Philips® Model TECNAI 20, OR, USA) with 80 kV accelerating voltage. The sample was prepared by dropping the solution on a copper grid and leave to dry prior to the investigation.

3.3.1.3.5 Hydrodynamic diameter, size distribution, and zeta potential

The attributes of the AuNPs were characterized considering the hydrodynamic diameter, size distribution, and zeta potential. A Zetasizer NanoZS (Malvern Instruments, UK) was used for the measurement. Before the measurements, the gold colloidal solutions were freshly prepared and diluted with purified water (1:9). The examination was performed in triplicate at 25 °C.

AuNPs formulations that were found to be red colloids with high intensity absorption (high yield) of maximum wavelength between 500-550 nm and has the particle size less than 100 nm with a narrow size distribution were considered to be with potentials and selected for further experiments.

3.3.1.4 Stability study of CS-AuNPs

The colloidal stability of CS-AuNPs prepared by both conventional heating and MW irradiation was investigated. The solutions were stored in a refrigerator at 4°C for 28 days. The physicochemical characteristics were evaluated and compared to the initial information for both conventional and MW method.

3.3.1.5 Preliminary study of metal binding property of CS-AuNPs

Brazilein is a phytochemical in CS extract that is able to bind to certain metal ions. The capability of CS-AuNPs to chelate mono- and polyvalent ions was investigated to determine the agglomeration state of the AuNPs upon ion binding which would alter the solution color. Briefly, 100 µL of 20 mM Fe^{2+} Fe^{3+} Al^{3+} K^+ Ca^{2+} Zn^{2+} Mg^{2+} solution which were prepared from $\text{FeSO}_4 \cdot 7\text{H}_2\text{O}$, $\text{FeCl}_3 \cdot 6\text{H}_2\text{O}$, $\text{Al}_2(\text{SO}_4)_3 \cdot 18\text{H}_2\text{O}$,

K_2SO_4 , $CaSO_4 \cdot 2H_2O$, $ZnSO_4 \cdot 7H_2O$, $MgSO_4 \cdot 7H_2O$, respectively, were mixed with 100 μ L of CS-AuNPs solution. The reaction was allowed to perform at room temperature for 10 min. Then, the color change and UV absorption spectra were evaluated to illustrate any shift of the maximum wavelength.

3.3.2 Chitosan-capped gold nanoparticles (CTS-AuNPs)

3.3.2.1 MW-assisted synthesis of CTS-AuNPs

The CTS-AuNPs were synthesized using MW-assisted technique. In brief, 10 mM $HAuCl_4$ solution was prepared and 0.75 mL of the solution was added to a 10-mL reaction vessel and mixed with 5 mL of 0.1 % w/v CTS in 1 % v/v acetic acid. The vessel was then placed in the MW synthesizer and a fixed temperature mode was turned on. The temperature was varied from 105, 125, and 145 °C, and the reaction time was varied from 20, 40, and 60 s to optimize the AuNPs synthesis. The resulting solutions were instantly cooled by immersing in an ice bath after the reaction time ends to stop the reaction. Thereafter, the synthesized CTS-AuNPs were kept in a refrigerator until required.

3.3.2.2 Characterizations of CTS-AuNPs

3.3.2.2.1 Physical appearance

The physical appearance of CTS-AuNPs were examined visually as mentioned in the section 3.3.1.3.1.

3.3.2.2.2 Surface plasmon resonance effect

The surface plasmon resonance bands of CTS-AuNPs were collected using the method mentioned in the section 3.3.1.3.2.

3.3.2.2.3 Fourier-transform infrared spectroscopy

The chemical characteristics of CTS-AuNPs were investigated using FTIR measurement. The samples were prepared using a KBr disc technique. The AuNPs were collected by centrifugation of the solution at 14,800 rpm for 10 min. Then, the precipitate was obtained for washing with ultrapure water and dried overnight at 50 °C. The spectrum was compared with that collected from CTS extract.

3.3.2.2.4 Morphology and particle size of CTS-AuNPs

The CTS-AuNPs morphology and the particle size were studied using the method mentioned in the section 3.3.1.3.4.

3.3.2.2.5 Hydrodynamic diameter, size distribution, and zeta potential

The physicochemical characteristics of CTS-AuNPs were collected and the criteria for the section of the AuNPs appropriate for further investigations were as mentioned in the section 3.3.1.3.5.

3.3.2.3 *Development of the colorimetric assay for Na₂EDTA injection using CTS-AuNPs*

3.3.2.3.1 Assay procedure

Standard Na₂EDTA dihydrate powder were acquired for the preparation of standard solution series. By that, the standard compound was accurately weighed and dissolve in water then diluted to the following concentrations: 0.1, 0.2, 0.4, 0.6, 0.8, and 1.0 mM. Whereas, Na₂EDTA injection (150 mg/mL, eq. to 446 mM of Na₂EDTA) was used to prepare the sample solution at a final concentration of 0.5 mM. The analysis was performed in a 96-well plate by mixing 75 μ L of Na₂EDTA standard or sample solution with 100 μ L CTS-AuNPs solution (as prepared) and 25 μ L of Britton-Robinson buffer (pH 4). The mixtures were made homogeneous with a micropipette, then incubated at an ambient temperature for 10 min. The absorbance of each well was collected with a multimode microplate reader at 650 nm. The quantity of Na₂EDTA in the sample was calculated from the prepared standard curve.

3.3.2.3.2 Method validation

Analytical method validation was performed to affirm the performance of the proposed analytical method with CTS-AuNPs. The International Conference of Harmonization (ICH) guidelines (ICH Q2 (R1) (2005)) [104] was used as a reference for the analytical method validation procedures.

3.3.2.3.2.1 Linearity and range

The efficient analytical range that the drug concentration (independent variable) presented a linear relationship with the instrumental responses (dependent variable) was

determined. Seven concentrations of Na₂EDTA standard solutions varied between 0.1–1.2 mM were plotted against the absorption responses and an appropriate regression model in a SigmaPlot software was used to compute the coefficient of determination (r^2)

3.3.2.3.2.2 Limit of detection and limit of quantification

The limit of detection (LOD) and limit of quantitation (LOQ) which is described as 3.3 and 10 times the standard deviation of blank measurements (n=10), respectively, were calculated according to the regression analysis.

3.3.2.3.2.3 Accuracy

The accuracy of the analytical procedure was examined by the quantification of the Na₂EDTA standard solutions. Three known concentration levels composing of 0.4, 0.5, 0.6 mM were quantified each in triplicate using the proposed assay method. The %recovery of was calculated using the following equation.

$$\% \text{Recovery} = \frac{\text{Assayed Na}_2\text{EDTA content}}{\text{Known Na}_2\text{EDTA content}} \times 100$$

3.3.2.3.2.4 Intra-day and inter-day precision

By examining six injection samples in one day for three consecutive days, the intra-day and inter-day precision were evaluated, respectively. The relative standard deviation (%RSD) values of the replicates were used to express the variances in the assay results.

3.3.2.3.3 Comparison of the proposed method with the standard method

Commercially available edetate disodium injection was assayed using the proposed method and USP43 method (complexometric titration) [105] as the reference procedure. The quantification result was described as %labeled amount where the results were compared using t-test.

3.3.2.4 Recovery of gold from laboratory waste and composition analysis

To the colored liquid laboratory waste from the experiments, sodium hydroxide (3 M) solution was added while stirring until the pH reached to approximately 7. Upon adding the basic solution, CTS-AuNPs in the waste were aggregated and precipitated.

The waste solutions were then centrifuged to collect the precipitate where the clear supernatants were removed. Thereafter, the solid precipitates were placed in a porcelain dish and dried in an ambient atmosphere or in a hot air oven to recover high-purity gold from the AuNPs. Concentrated sulfuric acid was added to the completely dried solids and was then heated on a burner until no fume was seen to digest and eradicate other organic compounds. The recovered gold was observed as tiny grains on the dish.

The recovered gold from the laboratory waste was analyzed on the composition using scanning electron microscopy (SEM)–coupled with energy-dispersive X-ray spectroscopy. Briefly, the gold grain scratched from the dish was adhered on the SEM stub by a carbon double-sided adhesive tape. The information on the identity and purity of gold can be given from the analysis.

3.3.2.5 *Statistical analysis*

Unless stated with the respective method section, all experiments were performed in triplicate. The results were reported as mean \pm standard deviation. Statistical analysis of Student's *t*-tests were conducted using Microsoft® Excel. Statistic significant differences were noted where $p < 0.05$.



CHAPTER 4

RESULTS AND DISCUSSION

4.1 *Caesalpinia sappan* capped gold nanoparticles (CS-AuNPs)

4.1.1 MW-assisted extraction of CS heartwood

Reported by several literatures, organic solvents [85] or their mixtures with water i.e., ethanol/water [84, 106] have been utilized for the brazilin extraction from CS heartwood. In this research, the only extractant used was water in order to obtain an aqueous extract readily to be used in AuNPs synthesis; otherwise, the method would be less environmental-friendly and organic solvents removal process would be required. The MW-assisted extraction was used in this study due to its superior capability of naturally-derived material extraction. This method provides a faster and deeper internal heating compared to the conventional method which would yield a larger content of the active substance, brazilin. Different extraction parameters were studied composing of MW power and extraction time to establish the optimal extraction condition. The finding revealed that higher brazilin content was obtained when higher MW power and longer irradiation time were used (Figure 8(a)). Thus, the MW irradiation would terminate to avoid excess pressure generated in the synthesizer if additional time or MW power were given. Due to the limitation of the MW used, the condition of 300 W MW power and 3 min irradiation time was selected to be used for CS heartwood extraction in which $13.1 \pm 0.4\%$ w/w of brazilin was obtained.

Compared to the MW-assisted extraction, the conventional extraction method which was heating the samples in a water bath at 100°C provided significantly less brazilin content of $9.72 \pm 1.56\%$ w/w, as shown in Figure 8(b). Besides, the simple heating technique inquired over 10 times longer extraction time (30 min). This was reported to be due to the irradiation of MW range energy could create the disruption of the plant cells and allowed more efficient mass transfer of the extractant into the organelles [76, 83]. Subsequently, the active compounds are released and contained in the extraction fluid. Moreover, oxidation and degradation of brazilin to brazilein [83] could be avoided when shorter heating time was given. This resulted improved brazilin extraction effectiveness and yield higher amount of brazilin. Apart from that, the MW-assisted synthesis would provide superior batch-to-batch reproducibility for brazilin

extraction since the heating process is more trustworthy and the temperature can be precisely controlled. This can be observed by lower standard deviation values shown by the error bars of the brazilin content obtained from the MW-assisted method compared to the conventional heating method in Figure 8. This suggested that the MW-assisted extraction method is a more efficient and faster method for brazilin extraction. Thus, the method yielded an extract readily to be used for AuNPs synthesis in a far less time-consuming manner. Brazilin is a compound in the CS extract with known pharmacological activity. The method can be conveniently used to prepare the extract in an aqueous form and used for further studies for other medical applications.

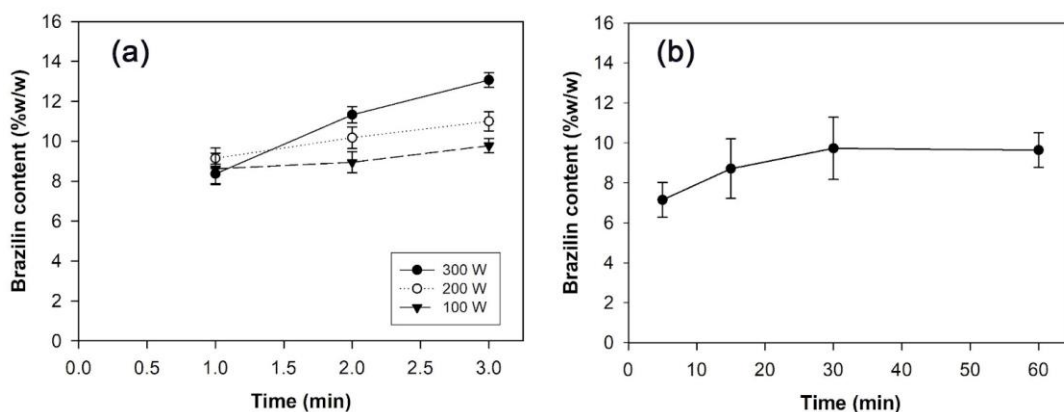


Figure 8 The amount of brazilin found in the CS extract delivered by (a) the MW-assisted method and (b) conventional heating method using 100°C temperature (n=3).

4.1.2 Optimal condition for MW-assisted synthesis and characteristics of CS-AuNPs

For the synthesis of CS-AuNPs with MW-mediated technique, the CS extraction as acquired from the MW-assisted extraction method was used. It is known that temperature has a significant effect towards AuNPs synthesis. Literatures reported that precise temperature control given by the MW function provided AuNPs with highly reproducible size and narrow size distribution [107]. Therefore, the Dynamic control mode on the MW synthesizer was selected to be used for AuNPs synthesis in this study. The dynamic control function allows the MW to titrate the temperature and hold at the level set by the user. This is done by a constant tune of the MW power during the

reaction period. To find the most suitable reacting condition, the system was set with the temperature of 60 °C for 1 min, and the volume of the prepared CS extract and the concentration of H_{AuCl}₄ solution were used.

The findings (Figure 9) presented that the varied reactant composition generates different colors of the colloidal solutions. Upon using low concentration of H_{AuCl}₄ (0.5 mM), the resulting solution was pale pink or yellow referring to low AuNPs content received. On the contrary, a darker solution of AuNPs was obtained if high concentration of H_{AuCl}₄ (2.5 mM) was initially used along with high amount of CS extract (400 and 600 μL). This was presumably caused by an excess amount of reduction functional groups of CS extract that may have affected the reaction, created side reactions among the gold ions resulting unwanted characteristics of AuNPs [18]. The reactions containing 5 mL of 1.5 mM H_{AuCl}₄ solution and 400 μL of the CS extract were promising for solutions with red-wine color and smallest AuNPs size were obtained. According to the gathered information, the MW irradiation parameters were then further varied. Though it was acknowledged that the time and temperature of the MW greatly impacted the AuNPs synthesis and attributes with different reducing agents, those factors were not as greatly affected the synthesized AuNPs as the composition given to the reaction [108-110]. Figure 10 showed that upon varying the synthesis time and MW temperature, the color of the resulting solutions was similar. Thus, the reaction performed with the temperature of 60°C and 1 min MW irradiation produced the smallest AuNPs size with low polydispersity index (PDI).

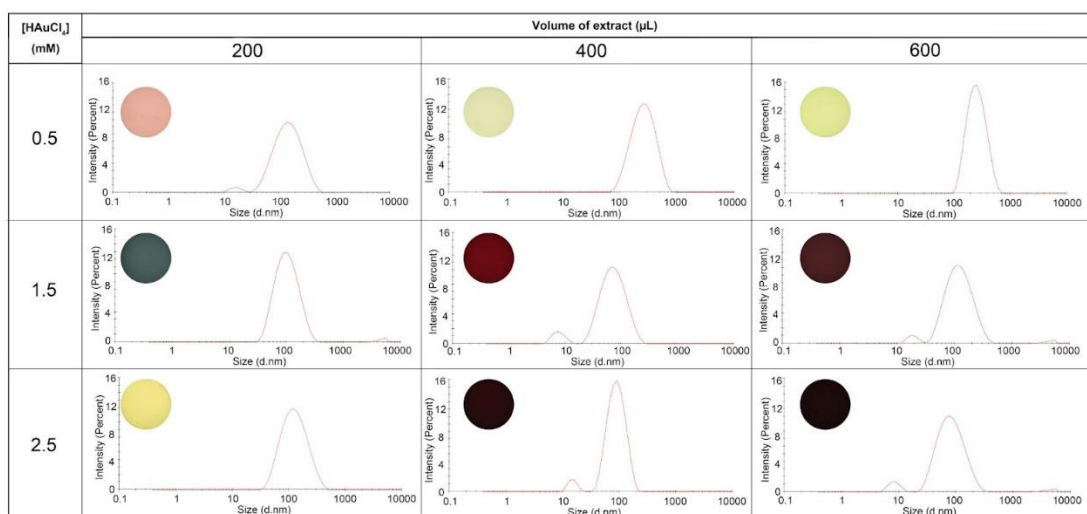


Figure 9 The solution color (shown in circle) and the particle size distribution of CS-AuNPs synthesized with different reactant compositions. Each reaction was performed using the MW-assisted method at the temperature of 60°C for 1 min.

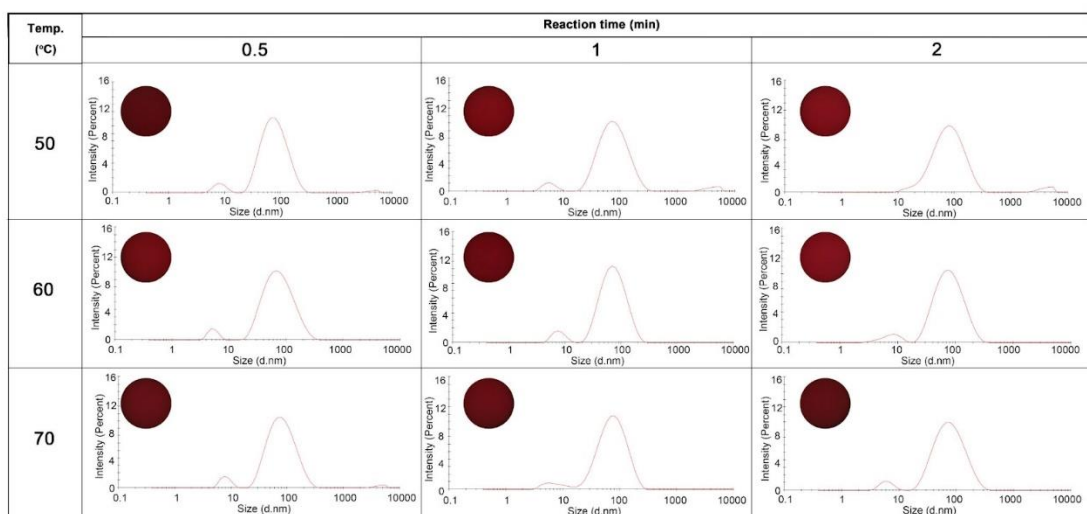


Figure 10 The solution color (shown in circle) and the particle size distribution of CS-AuNPs synthesized with varied time and temperature. Each reaction was performed using the MW-assisted method with 5 mL of 1.5 mM HAuCl₄ solution and 400 μL of the CS extract as the reactant.

The CS-AuNPs synthesized from the selected condition revealed a red-wine colored solution in which light scattering effect can be observed upon the given laser beam illustrating the colloidal properties of the CS-AuNPs solution (Figure 11(a)). Also, the UV-Vis absorption band of the AuNPs showed maximum absorption at 544 nm as presented in Figure 11(b). The TEM image of the AuNPs depicted a rather

spherical morphology with the mean diameter of 17.7 ± 4.4 nm (Figure 12). However, the hydrodynamic particle size of CS-AuNPs presented from the zetasizer was 49.6 ± 0.4 nm while the zeta potential was approximately -13.6 mV. The negative surface charge was presumably resulted from the charge of ionized brazilain and other phytochemical molecules such as phenolic compounds, flavonoids, or tannins that could be found in the CS extract used for AuNPs reduction and capping [85].

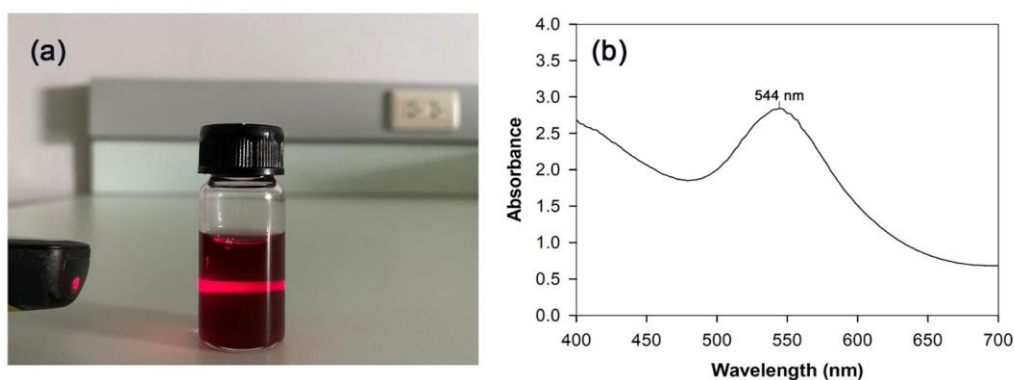


Figure 11 (a) The color of the resulting CS-AuNPs colloidal solution and light scattering Tyndall effect and (b) the scanned UV-Vis spectrum of CS-AuNP solution.

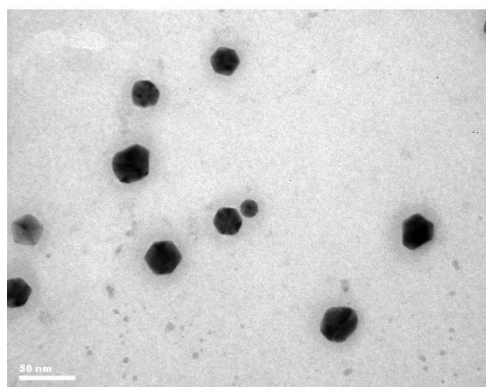


Figure 12 TEM image of CS-AuNPs.

The functional groups capped on the surface of the synthesized CS-AuNPs were confirmed by FTIR analysis. As shown in Figure 13, the spectra of both CS-AuNPs and CS extract presented the vibration of O–H stretching with a broad absorption band at 3400 cm^{-1} which also overlapped the 2923 cm^{-1} signal of C–H stretching. Considering the fingerprint region of the spectra, the absorption bands were similar for both samples.

A significant difference observed was the CS-AuNPs spectrum presented C=O stretching at 1507 cm^{-1} that was not seen on the CS extract spectrum. This carbonyl was attributed to brazilein that was oxidized from hydroxyl groups of brazilin [55]. Thus, it is certain that brazilein was the major phytochemical capped on the surface of CS-AuNPs.

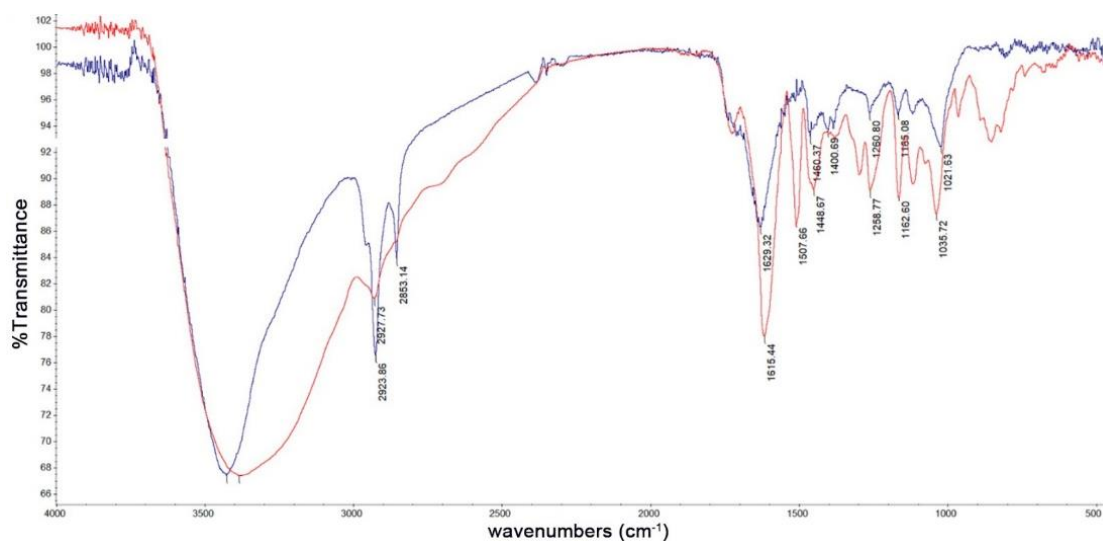


Figure 13 FTIR spectra of CS-AuNPs (red) and CS extract (blue).

Formerly, Chartarrayawadee et al. published the synthesis of CS-AuNPs prepared through the direct heating method [18]. The report stated that reconstituted freeze-dried CS extract obtained from 80°C heating for 3 h was added to the HAuCl_4 solution. The mixture was then mixed for 12 h before heated at 90°C for 1 h, and a combination of quasi-spherical and short-length earthworm-like shaped CS-AuNPs was acquired. These AuNPs were found to have average hydrodynamic size of 49 nm. Those AuNPs possessed the size comparable to the result in this study (50 nm) which used MW-assisted technique for CS extraction and AuNPs synthesis. Besides, the advantages of this findings were the rapid extraction of CS heartwood (3 min) as well as AuNPs synthesis (1 min) using the MW irradiation. Moreover, the CS extract can instantly be used without freeze-drying process for AuNPs synthesis after the extraction process and removal of plant debris. Therefore, it can be stated that MW-assisted method was a far more rapid and feasible technique compared to conventional heating.

4.1.3 Stability of CS-AuNPs

The synthesized CS-AuNPs were stored at 4°C for 28 days. The hydrodynamic particle size was then evaluated after the storage. It was found that the CS-AuNPs prepared using the MW-assisted method showed an increase in particle size from 49.6 ± 4.7 nm to 78.9 ± 13.2 nm as shown in Figure 14. However, the particle size was less than 100 nm which is a common definition of AuNPs. Concerning the CS-AuNPs obtained from the conventional preparation technique, the particle size of the AuNPs increased from 73.7 ± 5.4 nm to 134.7 ± 11.1 nm though the same reactant compositions and synthesis conditions were used. This suggested that the characteristics of CS-AuNPs could be different according to the heating method even if the other parameters were constant. Presumably, MW effects such as efficient heating or resulting material obtained after wave interactions and the dipolar polarization were given by the MW irradiation [108-110]. This results demonstrated that CS extract can be used as an efficient stabilizing agent of AuNPs with good stability in an appropriate condition over time. Also, the MW-assisted method could deliver CS-AuNPs with better stability compared to the conventional and convective heating method.

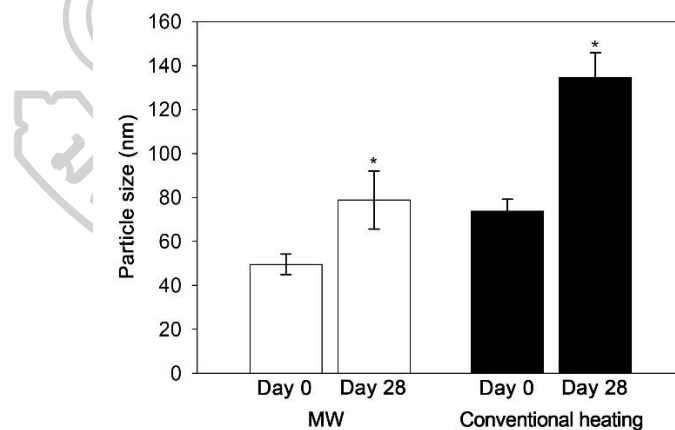


Figure 14 The mean of CS-AuNPs hydrodynamic particle size produced using MW irradiation versus conventional heating after 4°C for 28 days storage (n=3). *Signify statistically significant differences.

4.1.4 Metal ion binding property of CS-AuNPs

Brazilein has been reported that the compound was able to form coordination complex with some metal ions [89, 90]. So, the metal binding property of the synthesized CS-AuNPs was studied. To the CS-AuNPs solutions, Fe^{2+} , Fe^{3+} or Al^{3+}

were added. The color of the solutions was clearly changed from red to purple, while negligible changes were presented with other metal ions (Figure 15(a)). Moreover, a maximum absorption wavelength from 544 nm to 555 nm was observed with CS-AuNPs added with Fe^{2+} , Fe^{3+} or Al^{3+} as presented in Figure 15(b). The reason for the observed chromogenic and spectral changes was the agglomeration of CS-AuNPs caused by metal ions (Fe^{2+} , Fe^{3+} and Al^{3+}) binding proved by the TEM image shown in Figure 15(c). This discovery implicit that the CS-AuNPs were promising to be applied for selective detection of these ions in a formulation by means of colorimetric sensors. Formulations containing the stated metal ions such as antacid (aluminum hydroxide), ferrous sulfate supplements, and ions contaminated in water or other pharmaceutical products could be determined using the proposed CS-AuNPs. Nevertheless, further assay method, analytical method development, and method validation for AuNPs content as well as reaction condition optimization must be examined.

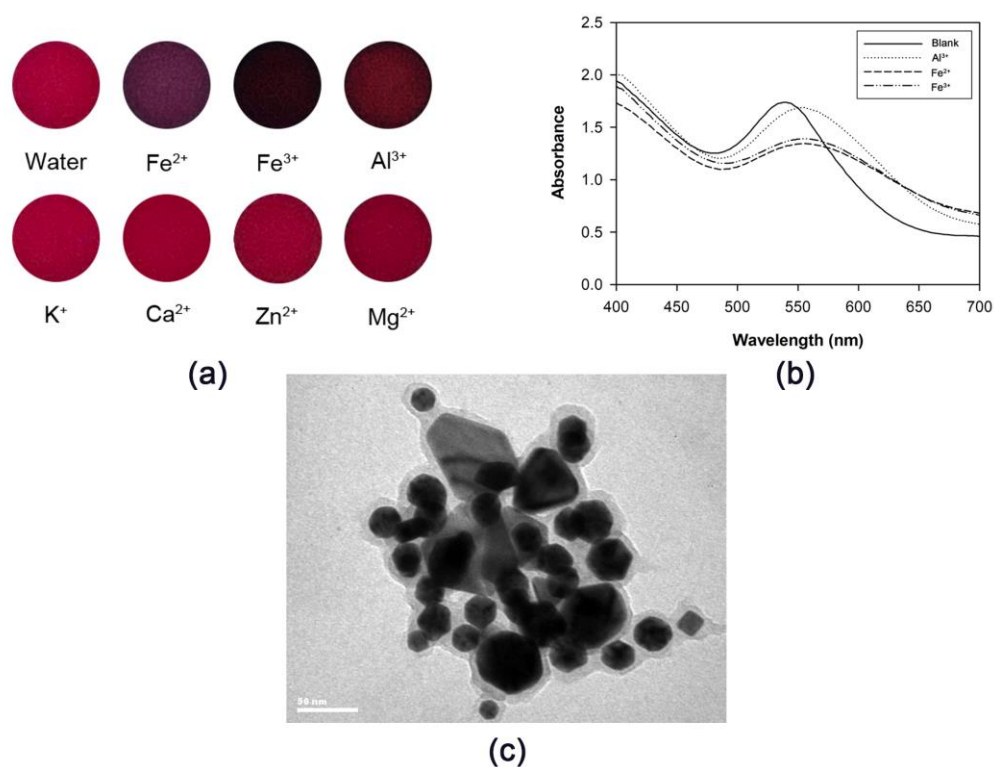


Figure 15 (a) Color of the CS-AuNPs solutions upon adding metal ions (blank measurement was performed in water), (b) UV-Vis absorption bands shift with added Fe^{2+} , Fe^{3+} or Al^{3+} , and (c) the observed CS-AuNPs agglomeration when Fe^{2+} was added under TEM.

4.2 Chitosan capped gold nanoparticles (CTS-AuNPs)

4.2.1 Optimization of MW-assisted CTS-AuNPs synthesis

For the synthesis of AuNPs using direct heating method, the temperature used to heat and catalyze the reaction was reported to have significant effect to the synthesis yield and the attribute of AuNPs. Therefore, heating temperature has been attentively monitored in the synthesis process of conventional heating [111, 112]. On the other hand, this factor has not been given very much interest when it comes to the use of MW-assisted method compared to the MW irradiation power. This study focused on the examination of the impact of the temperature used on the reaction for MW-assisted synthesis of CTS-AuNPs, also the suitable reacting temperature was optimized. Practically, the fixed temperature mode on the MW synthesizer was selected for the experiment. This operation mode allowed users to select the temperature control point and the operation run time which referred to the time held at the temperature programmed. The synthesizer would control the irradiation power of the instrument to deliver the temperature set.

The reacting solutions in all runs for synthesis optimization were fixed with 0.75 mL of 10 mM HAuCl₄ and 5 mL of 0.1 % w/v CTS solution. The temperature and reaction hold time was varied in search for the optimal synthesis condition. It was observed that after 1 min ramp period the color of all solutions went from yellow to ruby red within 10 s. This proved that AuNPs synthesis has occurred. Also, it was presented that the UV-Vis spectra of the CTS-AuNPs were altered with the change in maximum absorption wavelength and intensity once the reaction temperature was varied. Low CTS-AuNPs content was obtained if the solution was heated at 105 °C for 40 s as shown in Figure 16(a). It was suggested that the heating temperature was inadequate for AuNPs preparation. Obviously, higher CTS-AuNPs yield was received when the reaction temperature was increased to 125 °C for the reaction rate was improved. Apart from that, the resulted solution was a deep-red color, and the UV-Vis absorption band showed single and maximum absorption intensity at the wavelength of 520 nm. Considering the hold time set for the reaction while the synthesis temperature of 125 °C was kept, the time between 20 – 60 s did not show as much impact on the synthesis for no major changes on the light absorption spectra were noticed (Figure

16(b)). Yet, the hold time of 90 s resulted an agglomeration of AuNPs and their precipitation in the reaction vessel causing the loss of synthesis yield. Additionally, the narrowest surface plasmon resonance band in the shorter wavelength (blue region) was given when reaction was performed for 40 s referring to the small particle size AuNPs were formed. The color of AuNPs solution turned purplish-red after increasing the temperature to 145 °C. The spectrum from UV-Vis analysis was also amended as a new high intensity absorption was additionally observed at 650 nm. Former literature reports agreed that the reasons for such changes were the aggregation of AuNPs caused after overheating the reacting solution leading to particle size increase along with color alteration [113]. Larger particle size of the CTS-AuNPs synthesized at 145 °C was confirmed by DLS analysis which proved that the hydrodynamic particle size of CTS-AuNPs were greater than the AuNPs synthesized at 125 °C (Figure 17). Taking particle size and particle size in consideration, the synthesis using 125 °C temperature for 40 s seems to be optimal for CTS-AuNPs for delivering the uniformed small particle sizes.

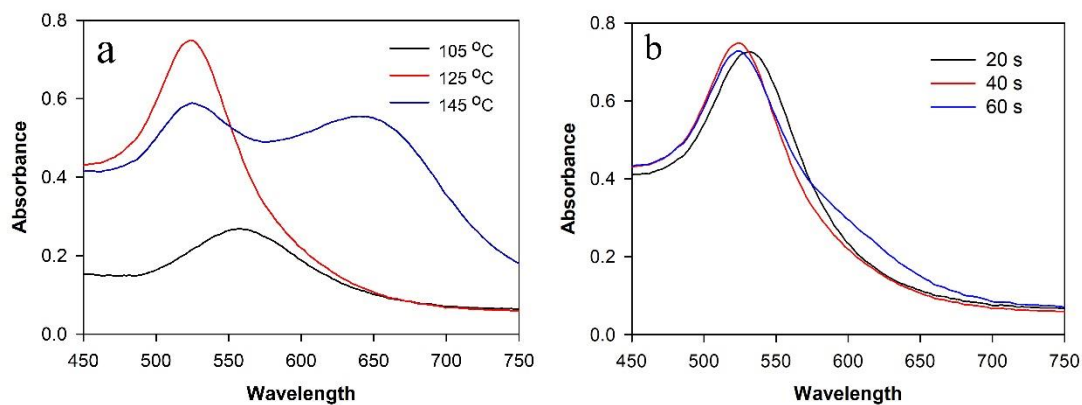


Figure 16 UV-Vis spectra of CTS-AuNPs synthesized with varied (a) reaction temperatures (time = 40 s) and (b) time (temperature = 125 °C).

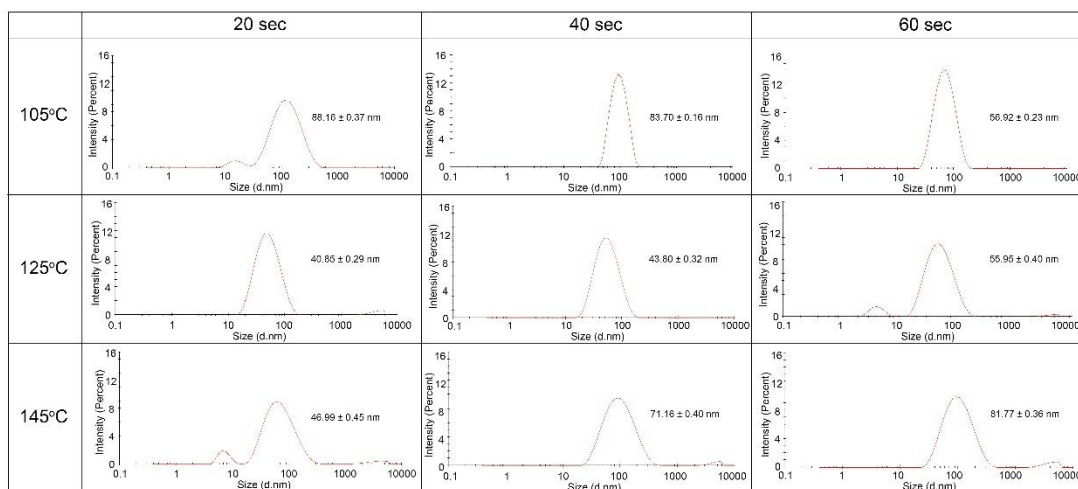


Figure 17 Particle size distribution determined by DLS technique of CTS-AuNPs synthesized with various reaction temperatures (rows) and time (column).

4.2.2 Characteristics of CTS-AuNPs

Once the optimal synthesis condition was used, CTS-AUNPs with a red colored solution with maximum absorption wavelength of 520 nm was obtained. Tyndall effect was conducted, and the colloidal property of the resulting solution was confirmed. The particle sized analyzed after TEM scrutinization was 17.8 ± 3.9 nm in average. Meanwhile, the DLC method established the mean hydrodynamic particle size of 43.8 nm with a fair size distribution showing PDI value of 0.32. The cause for distinct particle sized observed using two different method was likely to be due to the swelling property of CTS which was coated on the AuNPs. Highly positive zetapotential (30 mV) was found because CTS on the CTS-AuNPs surface was protonated at their primary amine moieties after dissolving in acidic environment used in the synthesis.

The capping of CTS on AuNPs was confirmed with FTIR measurement. In Figure 18, the broad absorption of O–H stretching overlapping N–H stretching presented at 3421 cm^{-1} and C–H stretching at 2923 cm^{-1} were presented on the spectrum of CTS. Also, the carbonyl groups of CTS showed a peak absorption from C=O stretching at 1646 cm^{-1} . Other major peaks found on CTS spectrum were 1567 and 1409 cm^{-1} which were attributed to the N–H bending of amine and 1074 cm^{-1} that belonged to the C–O stretching of the glycosidic linkage. On the other hand, similar absorption pattern was found on the CTS-AuNPs spectrum, thus some significant changes were

noticed. The C=O stretching at 1641 cm^{-1} were found to have higher intensity compared to CTS spectrum for Au^{3+} had oxidized the O–H functional groups of CTS to carbonyls. The amine bending shown at 1567 cm^{-1} also presented at a different wavenumber (1471 cm^{-1}) since the N–H vibration was decreased because CTS was bonded to AuNPs using the affinity interaction through the amines of CTS [43, 114]. Lastly, the decrease in the intensity of glycosidic linkage C–O stretching of CTS-AuNPs at 1072 cm^{-1} were found. This is likely because of a partial hydrolysis of the bond that may have occurred during the synthesis [115].

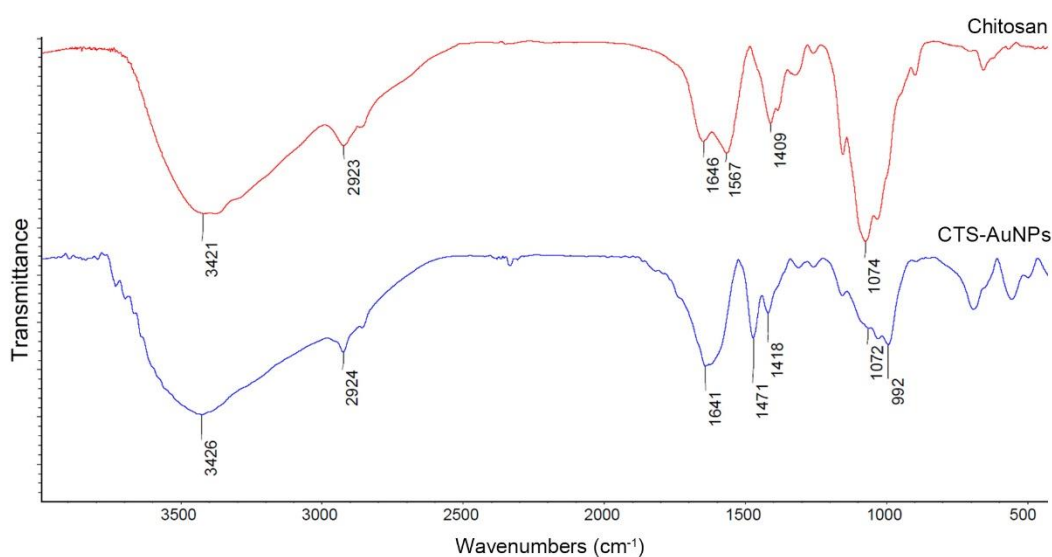


Figure 18 FTIR spectra of (a) chitosan (red) and (b) CTS-AuNPs (blue).

Several reports stated that CTS can be hydrolyzed in an acidic electrolytic solution after the MW irradiation was given. So, heating with MW power was proved to be efficient for the preparation of low molecular weight and oligomeric CTS because the hydrolytic deacetylation as well as CTS depolymerization can be accelerated with such condition [116, 117]. The hydrolysis rate was largely enhanced when halide salts like NaCl, KCl and MgCl_2 are present. This is probable for the conductivity and dielectric effect for MW coupling were improved [118]. Not only the MW irradiation showed superior efficacy on AuNPs synthesis, but also to other metal nanoparticles, like silver nanoparticles. The MW effect including wave interactions and the dipolar polarization phenomenon together with efficient heating offered by the MW synthesizer made the method a promising and attentive alternative synthesis method from the

conventional convective heating method [108-110]. Above all, the MW heating allowed rapid and efficient synthesis of uniform CTS-AuNPs. The active reducing species of CTS were generated after hydrolysis accelerated by the MW irradiation resulting homogenous nucleation and formation of CTS-AuNPs. Taking into account, the stability of CTS-AuNPs obtained was considerably desirable for significant changes were not noticed after 21-days storage at 4 °C.

The naturally derived polymer, CTS, was shown to be able to act as a green reducing agent and stabilizing agent for an efficient synthesis of CTS-AuNPs. The synthesis protocol proposed in this research can promisingly be used to prepare CTS-AuNPs for other applications. Besides, it is cautioned that the by-product, formic acid, could be formed from polymer hydrolysis and Au(III) oxidation which may be undesirable, though the synthesis reaction using CTS could be considered green and biocompatible [115, 119, 120]. Therefore, the amount of the by-product should be taken in consideration prior to using the CTS-AuNPs in biomedical application to endure safety of the product.

4.2.3 Analytical applicability of CTS-AuNPs

4.2.3.1 Principle of the colorimetric assay of edetate disodium

From the fact that CTS-AuNPs possesses primary amine of CTS on its surface, it can cause aggregation by interacting with polyanionic compounds through electrostatic interaction, thus the change of the solution color from red to blue can be noticed. This knowledge can be acquired to develop a colorimetric assay for certain analytes. Edetate disodium (Na_2EDTA) are used as a chelator or antidote for heavy metal poisoning. The molecule contains polycarboxylic groups that are used for metal ion binding. To control the quality of the product, pharmacopeial method for Na_2EDTA injection assay which is complexometric titration is widely used. The method composed of multiple preparation and analysis steps and utilize great amounts of reagents. Also, the simultaneous measurement of multiple samples or replicates are limited. The use of CTS-AuNPs can be applied to demonstrate the application of the synthesized product and could also overcome the disadvantages of the pharmacopeial method. So, the acquisition of CTS-AuNPs as the colorimetric sensor for Na_2EDTA injection assay was

developed to allow quantification of the compound through UV-Vis spectrophotometric analysis. The Figure 19 shows the reaction between Na_2EDTA and CTS-AuNPs that resulted the aggregation of the particles. Colorimetric change from red to blue solution that was caused by the shift of surface plasmon resonance band from 520 to 670 nm can be detected (Figure 20(a)). Also, the agglomeration among the CTS-AuNPs can be observed under TEM (Figure 20(b)-20(c)).

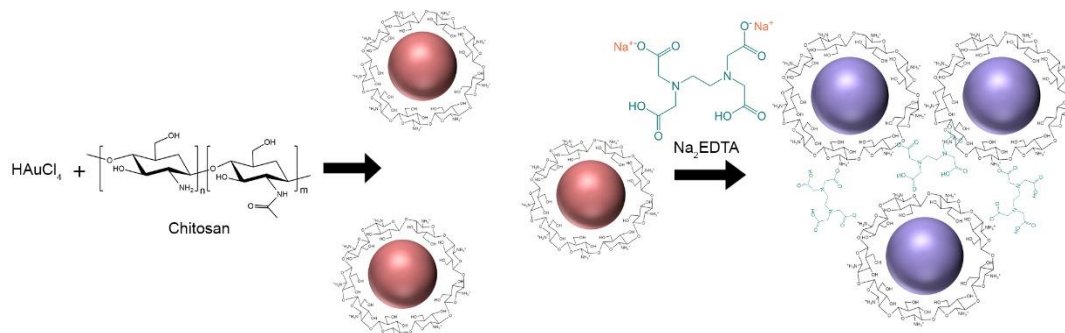


Figure 19 Suggested mechanism of colorimetric reaction occurred among CTS-AuNPs and Na_2EDTA .



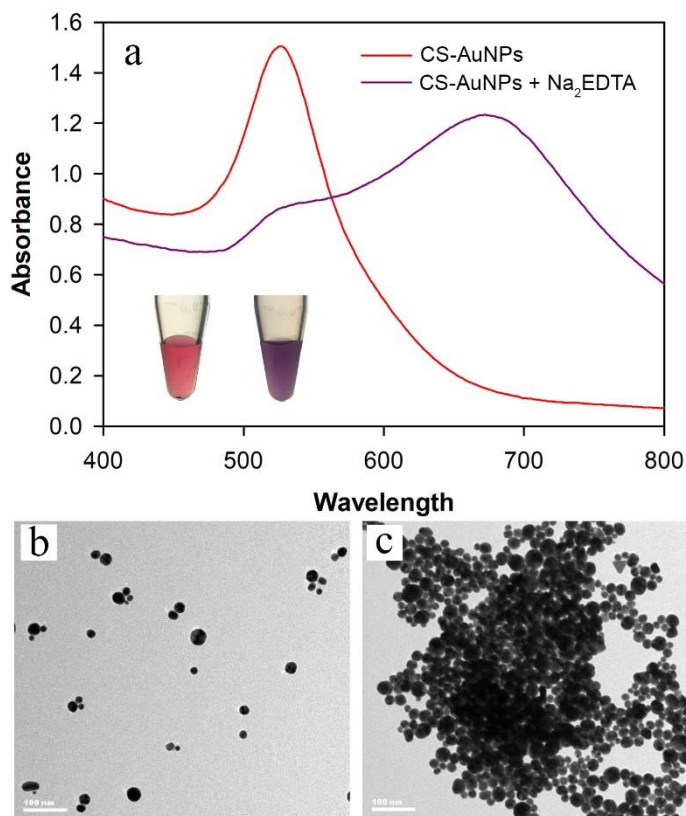


Figure 20 (a) UV-vis spectra of CTS-AuNPs (red) and the CTS-AuNPs interacted with Na_2EDTA (purple), and TEM images of (b) CTS-AuNPs and (c) CTS-AuNPs aggregation.

4.2.3.2 Assay conditions optimization

4.2.3.2.1 pH of the reaction

The optimal pH of the reaction was studied by primarily select the condition in which the CTS-AuNPs were stable. To the buffer of different pH values, the CTS-AuNPs were immersed to observe the change in the solution color. It was noted that the color of the solution turned from red to blue when the pH was slowly increase to pH = 5. The spectral change was also visible at this condition where the absorbance at 670 nm was greatly increased as shown in Figure 21(a). CTS is soluble in an acid medium with pH below its pKa value of 6.5 in which the polymer stays in its cationic form. Its aqueous solubility dropped drastically if the pH was raised to over 6.5 which would eventually cause the polymer precipitates. The capability of CTS to cap and stabilize the AuNPs was then declined and drove the AuNPs to form large aggregates. During the preliminary study, it was found the color of CTS-AuNPs solution could change if

the pH was greater than 5 though Na₂EDTA was not involved. The condition was unfortunately be accounted as inappropriate for the assay. Further examinations on Na₂EDTA assay with the CTS-AuNPs pH ranged from 2 to 4 revealed that the pH most suitable for the analysis was pH = 4. This was because the condition provided the most accurate correlation between the absorbance and the drug concentration (Figure 21(b)). EDTA are protonated when the pH was less than 3 created less negatively charged molecules to interact with the CTS-AuNPs that the change in the color of the solution was not clearly observed thus not suitable to be used for the analysis.

4.2.3.2.2 CTS-AuNPs solution volume

The concentration and the amount of CTS-AuNPs used in the reaction were considered a significant parameter to be studied to demonstrate the sensitivity of the method. Using the optimized pH of the solution (pH = 4), various volumes of the CTS-AuNPs as received from the synthesis added to the reaction mixtures were investigated. The Figure 21(c) presented that upon increasing the CTS-AuNPs volume to the reaction from 50 to 100 μ L, the absorbance and the slope of the standard curve increased and signified greater sensitivity of the analysis. However, the sensitivity considering the slope of the standard curve did not improve for showing a parallel curve to that of the 100 μ L when 150 μ L of the CTS-AuNPs was used. Therefore, the most suitable volume of CTS-AuNPs solution to be added to the reaction mixture was 100 μ L that yielded desirable sensitivity and minimized the use of reagents.

4.2.3.2.3 Reaction time

It was investigated that the reaction between CTS-AuNPs and Na₂EDTA took some time to occur and that the aggregations were formed. The shortest time required for the reaction to complete and gave the most intense color of the aggregated solution was studied. It is depicted in the Figure 21(d) that after mixing Na₂EDTA with CTS-AuNPs for 5 min the slope of the calibration curve was lower than other time points investigated suggesting that the reaction was not completed. Once the time used to incubate the mixture was given further to 10 and 20 min, the absorbance of the reaction was increased and higher slope of the curve was given. However, no significant

different between the slopes of the standard curve found for 10 min and 20 min were noticed. This stated that the reaction was completed after 10 min and was ready to be read and inquire for the assay. Moreover, the color remained stable until 20 min incubation. It was further observed that the developed color would fade down after incubating for 1 h because of the aggregated particles started to precipitate. So, the incubation time and read time for the assay between 10–20 min subsequent to reactant mixing were recommended to achieve reliable results.

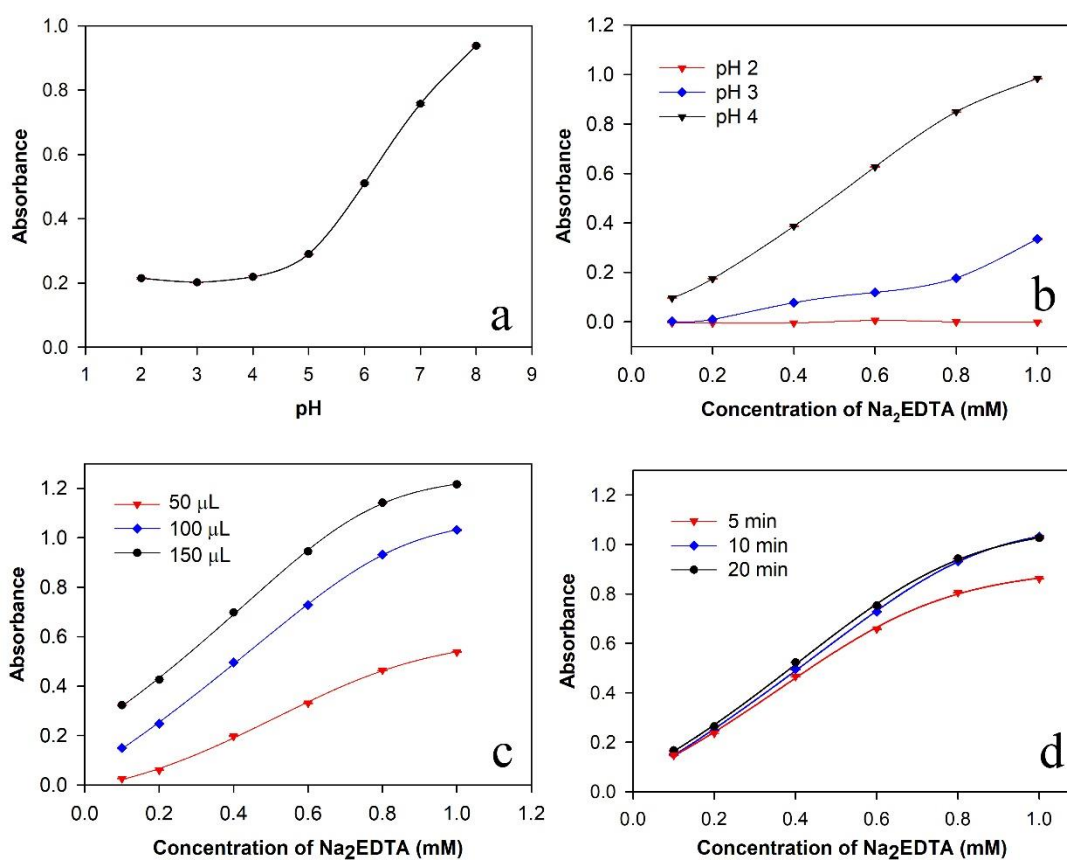


Figure 21 (a) The relationship between the absorbance and pH at a fixed wavelength of 670 nm. The relationship between the absorbance and Na₂EDTA concentration with the effect of (b) pH, (c) CTS-AuNPs volume, and (d) assay reaction time.

4.2.3.3 Analytical performance of the assay

Analytical method validation was performed after the optimized assay condition was determined. A suitable regression equation was used to demonstrate the relationship between the absorbance at 670 nm as the analytical signal and Na₂EDTA concentration. From the experiments, it was clear that the simple linear regression

seems to be inappropriate for the responses showed a S-shaped sigmoidal correlation curve. Thus, a non-linear regression model was required. According to the literature review, the observed curved-relationship was comparable to the responses received from the assay of different biological experiments such as immunoassays, dose-response curves, ligand binding assays, etc. that the responses were non-linear. The recommended models to be used for the analysis of this type of response were the 4-parameter logistic (4 PL) [121, 122] and 5-parameter logistic models [122]. A symmetrical S-shaped response curve best define the relationship found in this study, hence, the 4 PL regression equation was most suitable (table 1) to be used to describe the correlation and selected to explain the relationship of Na₂EDTA concentrations ranged between 0.1–1.2 mM.

The equation is shown as follows:

$$y = \min + \frac{(\max - \min)}{1 + \left(\frac{x}{EC_{50}}\right)^{-Hillslope}}$$

where y = the absorbance at 670 nm

x = the concentration of Na₂EDTA (mM)

min = 0.0910 (the minimum concentration)

max = 1.2792 (the maximum concentration)

EC₅₀ = 0.6386

Hillslope = 2.3777

Although, 5 PL regression equation had a higher R², the equation was too complicated for the calculation. Therefore, it was not chosen for use. (Table 1)

Table 1 Regression models representing the relationship of absorbance and concentration of Na₂EDTA

Regression model	Concentration range (mM)	R ²
Linear	0.1 – 0.8	0.9976
Linear	0.1 – 1.2	0.9785

Quadratic	0.1 – 1.2	0.9932
4-parameter logistic	0.1 – 1.2	0.9992
5-parameter logistic	0.1 – 1.2	1.0000

After the model fitting, the coefficient of determination (R^2) from the regression analysis was found to be 0.9992 when the concentration of Na_2EDTA ranged from 0.1–1.2 mM. The coefficient was very close to 1 stating an acceptable linearity. Considering other regression factors, the mean square error was 0.0003, the sum of squared residual was 0.0008, and the SD of the residuals was 0.0163 which illustrated that all the error concerning parameters were close to 0. Considering all the results found, the 4 PL model showed goodness of fit and was selected to describe the proposed assay for Na_2EDTA . Practically, the 4 PL model is known to be more complicated to be used compared to the simple linear model. Nowadays, there are several curve fitting and assay calculation software available both offline e.g., SigmaPlot and Assayfit Pro, Microsoft Excel add-in, and online e.g., MyAssays.com and MyCurveFit.com.

The colorimetric reaction between CTS-AuNPs and Na_2EDTA is shown in Figure 22(a). According to the calibration curve prepared, the LOD and LOQ for Na_2EDTA quantitative analysis were discovered to be 0.036 and 0.080 mM, respectively (Figure 22(b)). The accuracy of the method was considerably desirable with the percentages of recovery of 99.2%, 100.8%, and 101.6% for the concentration of Na_2EDTA 0.4, 0.5 and 0.6 mM, respectively. Each analysis was performed in triplicate. Six assay analyses were performed independently to determine the precision of the analysis method. The %RSD for intra-day precision was 1.1, while the inter-day precision was 1.47 which proved that the repeatability and reproducibility of the method was accountable. The method specificity was not conducted because the Na_2EDTA injection did not contain other compounds. However, this parameter needed to be further investigated when CTS-AuNPs would be acquired in the development for the analysis of other or more complicated formulations.

In this work, the analytical method with CTS-AuNPs was proposed and the analysis results were compared with the official pharmacopeial method for Na_2EDTA injection assay which is complexometric titration. The results revealed that the

%labeled amount of Na_2EDTA after 6 replicates were $100.67 \pm 0.68\%$ and $100.36 \pm 0.28\%$ from the proposed method and the official method, respectively. Subsequent to the statistical analysis using Student's *t*-test at 95% confidence level, no significant difference between the two results were found (calculated *t*-values = 1.018 and critical *t*-values = 2.365). All in all, the proposed method using CTS-AuNPs for the analysis of Na_2EDTA in its injection formulation was an attainable method to control the quality of the formulation. The advantages of this method were the rapid and simultaneous evaluation of multiple samples. Also, the method can be further developed to be used to control the quality of other polyanionic substances.

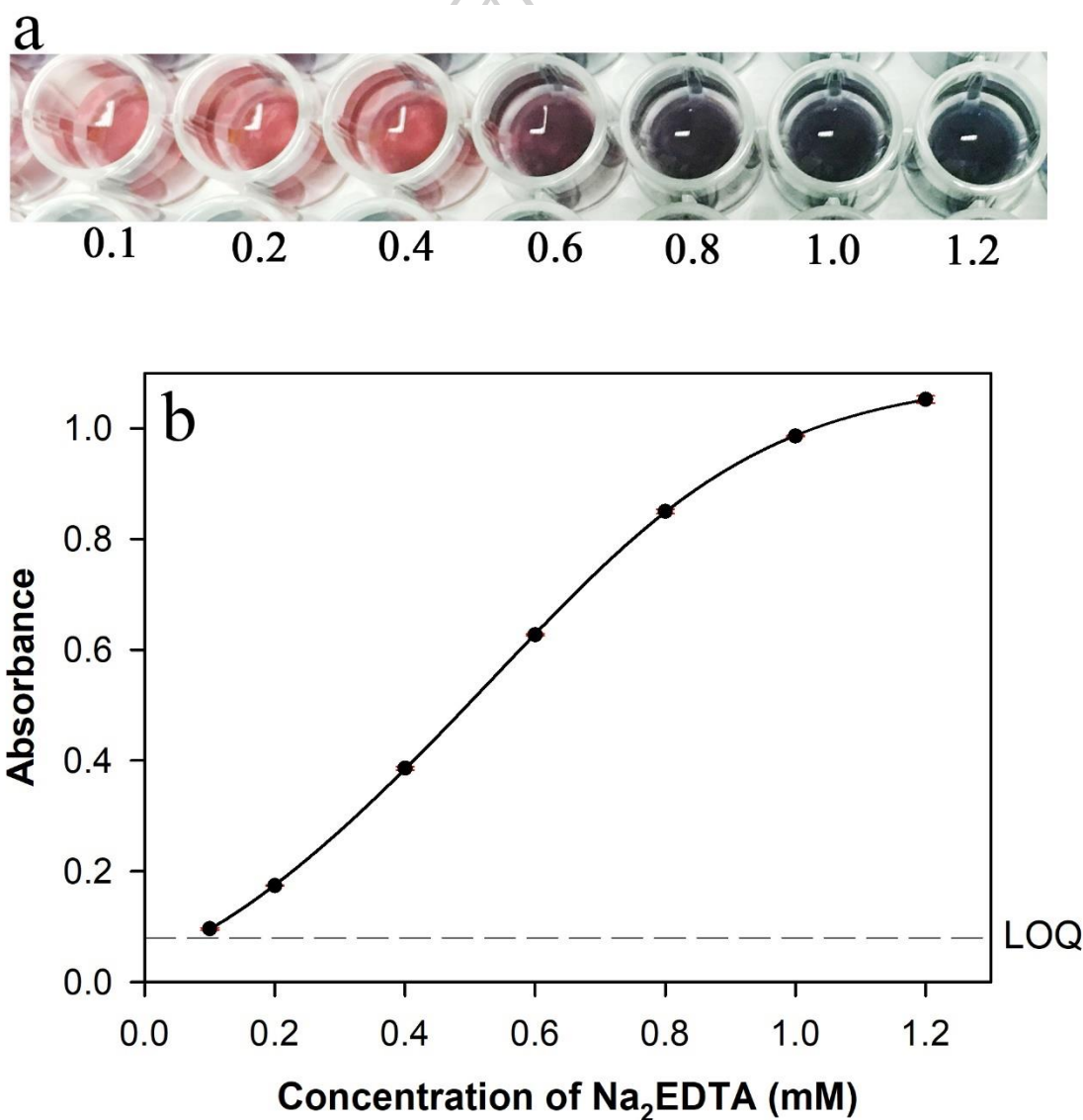


Figure 22 (a) The image of the colorimetric assay reaction with 0.1–1.2 mM Na_2EDTA and (b) a 4 PL standard curve showing the LOQ of 0.080 mM Na_2EDTA .

4.2.4 Laboratory waste treatment and gold recovery

In the emerging era of technologies, environmental impacts from the technology waste, including the those used in the biomedical applications have noted the interest of researchers. Metal nanoparticles, like AuNPs, leave metal wastes which is considered toxic even though the extent of these wastes is very low. Together with the metal nanoparticles, the ligands utilized with the drug delivery system are reported to be the major cause of environmental toxicity [123]. Some have reported that AuNPs also have caused harm to the environment, particularly with the aquatic organisms. This was because AuNP products and wastes were commonly discarded into the marine. A study from Dedeh et al. [124], stated that genome composition modifications and gene expression of fish tissues were triggered after the exposure to AuNPs. Moreover, those products and wastes showed an increase in acetylcholine esterase activity in fish brains by amending neurotransmission process. This phenomenon was not found to occur when exposed to gold ions, thus intensifying the toxic of gold once prepared into nanoparticles. Despite the fact the CTS which is a nontoxic biocompatible material was used as a reducing and stabilizing agent in this study, the toxicity of AuNPs cannot be neglected since the harm to human and environment was still not clarified. Proper disposal and waste management of CTS-AuNPs were required to diminish any potential hazards.

It was known from the experiments that CTS-AuNPs would precipitate when the pH of the colloidal solution was adjusted over 6.5. In this work, all wastes created were treated with basic solutions to tune the pH of the waste solutions to 7 at which the CTS-AuNPs were aggregated and can be conveniently removed after centrifugation. The treatment of AuNPs involved solutions method stated were proven to be effective for all kinds of wastes (CS- AuNPs, CTS- AuNPs + Na₂EDTA reaction products, and residual unreacted CTS-AuNPs) were seen to precipitate resulting the purplish solution to turn into an almost clear solution especially after centrifugation. Peculiarly, a thin layer of shiny gold was observed with the dark colored precipitates after centrifugation as shown in Figure 23(a). This was a unique event that occurred with the CTS-AuNPs and not with citrate-capped AuNPs. Precisely, after adjusting the pH of the waste

solutions to over 7, the sedimentation of AuNPs happened. The finding provided an insight that CTS was loosely capped on the surface of AuNPs compared to the citrate ions since it can be easily separated from the gold surface when the pH was risen.

The gold layer from waste management was further refined and recovered. The precipitates from treated CTS-AuNPs wastes were digested in acid and ignited to demolish other organic compounds and the by-products e.g., formic acid, formed after the synthesis. The recovered gold solids were considered visibly shiny as shown in Figure 23(b). The solid gold was further analyzed using SEM-EDS to ascertain the identity and purity of gold. The result showed that the recovered gold had a purity of 97.62% by weight (Figure 23(c)-23(d)). Not only that the efficient and feasible laboratory metal waste management was reported in this study, but also the recovery of gold from CTS-AuNPs wastes was reported for the first time. All in all, CTS-AuNPs can be accounted as an appealing material with various advantages biomedically and environmentally for its wastes can be simply managed and recycled into a high-value material. The use of CTS-AuNPs was considerably support environmental sustainability and economic feasibility.

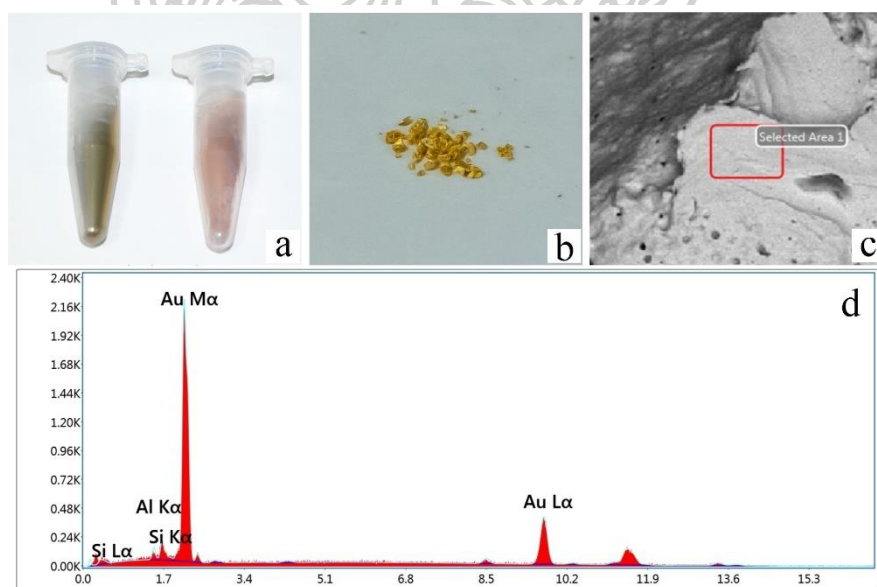


Figure 23 (a) The dried precipitates of CTS-AuNPs (left tube) and citrate-capped AuNPs (right tube) after the treatment with alkaline solution, (b) refined gold solids from CTS-AuNPs wastes, (c) SEM micrograph (top view) of gold grains, and (d) EDS spectrum of gold within the representative microscopic area marked with red-bordered rectangle in (c).

CHAPTER 5

CONCLUSION

5.1 Synthesis and application of CS-AuNPs

The extraction of CS heartwood using MW technology was described, as well as the subsequent fabrication of AuNPs using the extract as a reducing and stabilizing agent. With MW radiation, the extraction process took only three minutes, producing an extract with a high and consistent brazilin content that could be instantly employed to create AuNPs. Spherical CS-AuNPs with a nano-scaled size and acceptable stability were produced within 1 min under the optimal synthesis conditions, which included the reactant mixture, MW heating time, and reaction temperature. Additionally, the produced CS-AuNPs could selectively attach to Fe^{2+} , Fe^{3+} , and Al^{3+} and caused particle aggregation. Due to this occurrence, the color changed noticeably, and the UV-vis absorption maxima shifted, suggesting the possibility of colorimetric detection and quantitation of these metal ions.

5.2 Synthesis and application CTS-AuNPs

CTS was studied to be acquired as a reducing and stabilizing agent in a CTS-AuNPs synthesis process. The heating method used was MW irradiation in a fixed temperature mode, which has never been documented. In less than 2 min, the CTS-AuNPs with the desired nano-size, homogeneous size distribution, and light absorption capabilities were produced. CTS-AuNPs were used for the assay of Na_2EDTA injection based on the aggregation-induced color and absorption shift because of the positively charged surface interacting with the polyanions. The proposed validated method was easier, quicker, needed fewer chemicals, and could analyze a lot more samples than the currently employed titrimetric method. Furthermore, a simple laboratory process was developed and used to successfully transform the CTS-AuNPs wastes into products.

REFERENCES

1. K. Akshaya, C. Arthi, A. J. Pavithra, P. Poovizhi, S. S. Antinate, G. S. Hikku, K. Jeyasubramanian, R. Murugesan. Bioconjugated gold nanoparticles as an efficient colorimetric sensor for cancer diagnostics. *PHOTODIAGN PHOTODYN.* 30 (2020): 101699.
2. K. Kalimuthu, B. S. Cha, S. Kim, K. S. Park. Eco-friendly synthesis and biomedical applications of gold nanoparticles: A review. *MICROCHEM J.* 152 (2020): 104296.
3. B. Liu, J. Liu. Interface-driven hybrid materials based on dna-functionalized gold nanoparticles. *MATTER.* 1 (4) (2019): 825-47.
4. T. Khan, N. Ullah, M. A. Khan, Z.-u.-R. Mashwani, A. Nadhman. Plant-based gold nanoparticles; a comprehensive review of the decade-long research on synthesis, mechanistic aspects and diverse applications. *ADV COLLOID INTERFAC.* 272 (2019): 102017.
5. J. Santhoshkumar, S. Rajeshkumar, S. Venkat Kumar. Phyto-assisted synthesis, characterization and applications of gold nanoparticles – a review. *BIOCHEM BIOPHYS REP.* 11 (2017): 46-57.
6. M. Teimouri, F. Khosravi-Nejad, F. Attar, A. A. Saboury, I. Kostova, G. Benelli, M. Falahati. Gold nanoparticles fabrication by plant extracts: Synthesis, characterization, degradation of 4-nitrophenol from industrial wastewater, and insecticidal activity – a review. *J CLEAN PROD.* 184 (2018): 740-53.
7. T. Bu, M. Zhang, X. Sun, Y. Tian, F. Bai, P. Jia, Y. Bai, T. Zhe, L. Wang. Gold nanoparticles-functionalized microorganisms assisted construction of immunobiosensor for sensitive detection of ochratoxin a in food samples. *SENSOR ACTUAT B-CHEM.* 299 (2019): 126969.
8. M. P. Patil, G.-D. Kim. Marine microorganisms for synthesis of metallic nanoparticles and their biomedical applications. *COLLOID SURFACE B.* 172 (2018): 487-95.
9. R. Augustine, A. Hasan. Emerging applications of biocompatible phytosynthesized metal/metal oxide nanoparticles in healthcare. *J DRUG DELIV SCI TEC.* 56 (2020): 101516.
10. M. E. El-Naggar, T. I. Shaheen, M. M. G. Fouda, A. A. Hebeish. Eco-friendly microwave-assisted green and rapid synthesis of well-stabilized gold and core-shell silver-gold nanoparticles. *CARBOHYD POLYM.* 136 (2016): 1128-36.
11. K. A. Kumari, G. B. Reddy, V. Mittapalli. Microwave assisted synthesis of gold nanoparticles with *phyla nodiflora* (l.) greene leaves extract and its studies of catalytic reduction of organic pollutants. *MATER TODAY-PROC.* (2020).
12. M. Morad, M. A. Karim, H. M. Altass, A. E. R. S. Khder. Microwave-assisted synthesis of gold nanoparticles supported on mn_3o_4 catalyst for low temperature co oxidation. *ENVIRON TECHNOL.* (2019): 1-10.
13. N. P. Nirmal, M. S. Rajput, R. G. Prasad, M. Ahmad. Brazilin from *caesalpinia sappan* heartwood and its pharmacological activities: A review. *ASIAN PAC J TROP MED.* 8 (6) (2015): 421-30.
14. C. E. da Silva, P. Vandenabeele, H. G. M. Edwards, L. F. Cappa de Oliveira. Nif-raman spectroscopic analytical characterization of the fruits, seeds, and phytotherapeutic oils from rosehips. *ANAL BIOANAL CHEM.* 392 (7) (2008): 1489-96.

15. B. M. Choi, J. A. Lee, S. S. Gao, S. Y. Eun, Y. S. Kim, S. Y. Ryu, Y. H. Choi, R. Park, D. Y. Kwon, B. R. Kim. Brazilin and the extract from *caesalpinia sappan* l. Protect oxidative injury through the expression of heme oxygenase-1. *Biofactors*. 30 (3) (2007): 149-57.
16. N. P. Nirmal, P. Panichayupakaranant. Antioxidant, antibacterial, and anti-inflammatory activities of standardized brazilin-rich *caesalpinia sappan* extract. *PHARM BIOL*. 53 (9) (2015): 1339-43.
17. Y. Gao, L. Torrente-Murciano. Mechanistic insights of the reduction of gold salts in the turkevich protocol. *Nanoscale*. 12 (4) (2020): 2740-51.
18. W. Chartarrayawadee, C. O. Too, S. Ross, G. M. Ross, K. Jumpatong, A. Noimou, A. Settha. Green synthesis and stabilization of earthworm-like gold nanostructure and quasi-spherical shape using *caesalpinia sappan* linn. Extract. *GREEN PROCESS SYNTH*. 7 (5) (2018): 424-32.
19. S. Suvarna, U. Das, S. Kc, S. Mishra, M. Sudarshan, K. D. Saha, S. Dey, A. Chakraborty, Y. Narayana. Synthesis of a novel glucose capped gold nanoparticle as a better theranostic candidate. *PLoS One*. 12 (6) (2017): e0178202.
20. K. Shrivastava, N. Nirmalkar, S. S. Thakur, M. K. Deb, S. S. Shinde, R. Shankar. Sucrose capped gold nanoparticles as a plasmonic chemical sensor based on non-covalent interactions: Application for selective detection of vitamins b1 and b6 in brown and white rice food samples. *FOOD CHEM*. 250 (2018): 14-21.
21. X. Chen, X. Zhao, Y. Gao, J. Yin, M. Bai, F. Wang. Green synthesis of gold nanoparticles using carrageenan oligosaccharide and their in vitro antitumor activity. *Mar Drugs*. 16 (8) (2018): 277.
22. E.-K. Lim, E. Jang, J. Kim, T. Lee, E. Kim, H. S. Park, J.-S. Suh, Y.-M. Huh, S. Haam. Self-fabricated dextran-coated gold nanoparticles using pyrenyl dextran as a reducible stabilizer and their application as ct imaging agents for atherosclerosis. *J MATER CHEM*. 22 (34) (2012): 17518-24.
23. K. Wongmanee, S. Khuanamkam, S. Chairam. Gold nanoparticles stabilized by starch polymer and their use as catalyst in homocoupling of phenylboronic acid. *J KING SAUD UNIV SCI*. 29 (4) (2017): 547-52.
24. V. Kattumuri, M. Chandrasekhar, S. Guha, K. Raghuraman, K. V. Katti, K. Ghosh, R. J. Patel. Agarose-stabilized gold nanoparticles for surface-enhanced raman spectroscopic detection of DNA nucleosides. *APPL PHYS LETT*. 88 (15) (2006): 153114.
25. S. Dhar, V. Mali, S. Bodhankar, A. Shiras, B. L. V. Prasad, V. Pokharkar. Biocompatible gellan gum-reduced gold nanoparticles: Cellular uptake and subacute oral toxicity studies. *J APPL TOXICOL*. 31 (5) (2011): 411-20.
26. R. M. Devendiran, S. k. Chinnaiyan, N. K. Yadav, G. K. Moorthy, G. Ramanathan, S. Singaravelu, U. T. Sivagnanam, P. T. Perumal. Green synthesis of folic acid-conjugated gold nanoparticles with pectin as reducing/stabilizing agent for cancer theranostics. *RSC ADV*. 6 (35) (2016): 29757-68.
27. H. Kim, V. P. Nguyen, P. Manivasagan, M. J. Jung, S. W. Kim, J. Oh, H. W. Kang. Doxorubicin-fucoidan-gold nanoparticles composite for dual-chemo-photothermal treatment on eye tumors. *Oncotarget*. 8 (69) (2017): 113719-33.
28. H. Huang, X. Yang. Synthesis of chitosan-stabilized gold nanoparticles in the absence/presence of tripolyphosphate. *Biomacromolecules*. 5 (6) (2004): 2340-6.

29. M. Potara, D. Maniu, S. Astilean. The synthesis of biocompatible and sers-active gold nanoparticles using chitosan. *Nanotechnology*. 20 (31) (2009): 315602.
30. I.-C. Sun, C.-H. Ahn, K. Kim, S. Emelianov. Photoacoustic imaging of cancer cells with glycol-chitosan-coated gold nanoparticles as contrast agents. *J BIOMED OPT.* 24 (12) (2019): 121903.
31. D. S. Salem, M. A. Sliem, M. El-Sesy, S. A. Shouman, Y. Badr. Improved chemo-photothermal therapy of hepatocellular carcinoma using chitosan-coated gold nanoparticles. *J PHOTOCH PHOTOBIO B.* 182 (2018): 92-9.
32. P. Abrica-González, J. A. Zamora-Justo, A. Sotelo-López, G. R. Vázquez-Martínez, J. A. Balderas-López, A. Muñoz-Diosdado, M. Ibáñez-Hernández. Gold nanoparticles with chitosan, n-acylated chitosan, and chitosan oligosaccharide as DNA carriers. *Nanoscale Res Lett.* 14 (1) (2019): 258-.
33. P. Manivasagan, S. Bharathiraja, N. Q. Bui, I. G. Lim, J. Oh. Paclitaxel-loaded chitosan oligosaccharide-stabilized gold nanoparticles as novel agents for drug delivery and photoacoustic imaging of cancer cells. *INT J PHARM.* 511 (1) (2016): 367-79.
34. Z. Chen, Z. Wang, X. Chen, H. Xu, J. Liu. Chitosan-capped gold nanoparticles for selective and colorimetric sensing of heparin. *J NANOPART RES.* 15 (9) (2013): 1930.
35. C. Jiang, J. Zhu, Z. Li, J. Luo, J. Wang, Y. Sun. Chitosan-gold nanoparticles as peroxidase mimic and their application in glucose detection in serum. *RSC ADV.* 7 (70) (2017): 44463-9.
36. A. C. Martínez-Torres, D. G. Zarate-Triviño, H. Y. Lorenzo-Anota, A. Ávila-Ávila, C. Rodríguez-Abrego, C. Rodríguez-Padilla. Chitosan gold nanoparticles induce cell death in hela and mcf-7 cells through reactive oxygen species production. *INT J NANOMED.* (13) (2018): 3235-50.
37. C. O. Mohan, S. Gunasekaran, C. N. Ravishankar. Chitosan-capped gold nanoparticles for indicating temperature abuse in frozen stored products. *NPJ SCI FOOD.* 3 (1) (2019): 2.
38. M. R. A. Rovais, B. Alirezapour, M. E. Moasses, M. Amiri, F. B. Novin, E. Maadi. Internalization capabilities of gold-198 nanoparticles: Comparative evaluation of effects of chitosan agent on cellular uptake into mcf-7. *APPL RADIAT ISOTOPE.* 142 (2018): 85-91.
39. Sonia, Komal, S. Kukreti, M. Kaushik. Exploring the DNA damaging potential of chitosan and citrate-reduced gold nanoparticles: Physicochemical approach. *INT J BIOL MACROMOL.* 115 (2018): 801-10.
40. L. Sun, J. Li, J. Cai, L. Zhong, G. Ren, Q. Ma. One pot synthesis of gold nanoparticles using chitosan with varying degree of deacetylation and molecular weight. *CARBOHYD POLYM.* 178 (2017): 105-14.
41. V. Madhavan, P. K. Gangadharan, A. Ajayan, S. Chandran, P. Raveendran. Microwave-assisted solid-state synthesis of au nanoparticles, size-selective speciation, and their self-assembly into 2d-superlattice. *NANO-STRUCT NANO-OBJECTS.* 17 (2019): 218-22.
42. C. Fan, W. Li, S. Zhao, J. Chen, X. Li. Efficient one pot synthesis of chitosan-induced gold nanoparticles by microwave irradiation. *MATER LETT.* 62 (20) (2008): 3518-20.

43. A. Komalam, L. G. Muraleegharan, S. Subburaj, S. Suseela, A. Babu, S. George. Designed plasmonic nanocatalysts for the reduction of eosin y: Absorption and fluorescence study. INT NANO LETT. 2 (1) (2012): 26.
44. P. Sadhu, A. Rajput, A. Kumar, D. Dash, N. Shah, M. Kumari, S. Patel. A combined approach of gold nanoparticles with cannabinoids for the treatment of cancer - a review. INT J PHARM RES. 12 (2020): 393-405.
45. N. Z. A. Naharuddin, A. R. Sadrolhosseini, M. H. Abu Bakar, N. Tamchek, M. A. Mahdi. Laser ablation synthesis of gold nanoparticles in tetrahydrofuran. OPT MATER EXPRESS. 10 (2) (2020): 323-31.
46. M. Sengani, A. M. Grumezescu, V. D. Rajeswari. Recent trends and methodologies in gold nanoparticle synthesis – a prospective review on drug delivery aspect. OPENNANO. 2 (2017): 37-46.
47. J. Kimling, M. Maier, B. Okenve, V. Kotaidis, H. Ballot, A. Plech. Turkevich method for gold nanoparticle synthesis revisited. J PHYS CHEM B. 110 (32) (2006): 15700-7.
48. E. O. Mikhailova. Gold nanoparticles: Biosynthesis and potential of biomedical application. J FUNCT BIOMATER. 12 (4) (2021): 70.
49. S. He, Z. Guo, Y. Zhang, S. Zhang, J. Wang, N. Gu. Biosynthesis of gold nanoparticles using the bacteria *rhodopseudomonas capsulata*. MATER LETT. 61 (18) (2007): 3984-7.
50. X. Zhang, Y. Qu, W. Shen, J. Wang, H. Li, Z. Zhang, S. Li, J. Zhou. Biogenic synthesis of gold nanoparticles by yeast *magnusiomyces ingens* lh-f1 for catalytic reduction of nitrophenols. COLLOID SURFACE A. 497 (2016): 280-5.
51. P. Vijaya Kumar, S. Mary Jelastin Kala, K. S. Prakash. Green synthesis of gold nanoparticles using *croton caudatus geisel* leaf extract and their biological studies. MATER LETT. 236 (2019): 19-22.
52. S. S. Shankar, A. Ahmad, R. Pasricha, M. Sastry. Bioreduction of chloroaurate ions by geranium leaves and its endophytic fungus yields gold nanoparticles of different shapes. J MATER CHEM. 13 (7) (2003): 1822-6.
53. P. P. Gan, S. H. Ng, Y. Huang, S. F. Y. Li. Green synthesis of gold nanoparticles using palm oil mill effluent (pome): A low-cost and eco-friendly viable approach. BIORESOURCE TECHNOL. 113 (2012): 132-5.
54. D. Dhamecha, S. Jalalpure, K. Jadhav, S. Jagwani, R. Chavan. Doxorubicin loaded gold nanoparticles: Implication of passive targeting on anticancer efficacy. PHARMACOL RES. 113 (2016): 547-56.
55. R. de Oliveira, P. Zhao, N. Li, L. C. de Santa Maria, J. Vergnaud, J. Ruiz, D. Astruc, G. Barratt. Synthesis and in vitro studies of gold nanoparticles loaded with docetaxel. INT J PHARM. 454 (2) (2013): 703-11.
56. M. M. Encabo-Berzosa, M. Sancho-Albero, V. Sebastian, S. Irusta, M. Arruebo, J. Santamaria, P. Martín Duque. Polymer functionalized gold nanoparticles as nonviral gene delivery reagents. J GENE MED. 19 (6-7) (2017): e2964.
57. F. Lu, T. L. Doane, J.-J. Zhu, C. Burda. Gold nanoparticles for diagnostic sensing and therapy. INORG CHIM ACTA. 393 (2012): 142-53.
58. C. Zhao, L. Niu, X. Wang, W. Sun. Electrochemiluminescence of gold nanoparticles and gold nanoparticle-labelled antibodies as co-reactants. RSC ADV. 8 (63) (2018): 36219-22.

59. Y. Cheng, T. Stakenborg, P. Van Dorpe, L. Lagae, M. Wang, H. Chen, G. Borghs. Fluorescence near gold nanoparticles for DNA sensing. *ANAL CHEM.* 83 (4) (2011): 1307-14.
60. D. C. Hone, P. I. Walker, R. Evans-Gowing, S. FitzGerald, A. Beeby, I. Chambrier, M. J. Cook, D. A. Russell. Generation of cytotoxic singlet oxygen via phthalocyanine-stabilized gold nanoparticles: A potential delivery vehicle for photodynamic therapy. *Langmuir.* 18 (8) (2002): 2985-7.
61. S. A. C. Carabineiro. Supported gold nanoparticles as catalysts for the oxidation of alcohols and alkanes. *FRONT CHEM.* 7 (2019).
62. T. Mitsudome, K. Kaneda. Gold nanoparticle catalysts for selective hydrogenations. *GREEN CHEM.* 15 (10) (2013): 2636-54.
63. T. Lou, L. Chen, C. Zhang, Q. Kang, H. You, D. Shen, L. Chen. A simple and sensitive colorimetric method for detection of mercury ions based on anti-aggregation of gold nanoparticles. *ANAL METHODS-UK.* 4 (2) (2012): 488-91.
64. M. R. Hormozi-Nezhad, M. Azargun, N. Fahimi-Kashani. A colorimetric assay for d-penicillamine in urine and plasma samples based on the aggregation of gold nanoparticles. *J IRAN CHEM SOC.* 11 (5) (2014): 1249-55.
65. N. Esmaili, M. R. Sohrabi, F. Motiee. A simple, selective, and fast colorimetric assay using gold nanoparticles for trace determination of tolyltriazole in aqueous media. *IRAN J CHEM CHEM ENG.* 40 (1) (2021): 49-56.
66. P. Pati, S. McGinnis, P. J. Vikesland. Waste not want not: Life cycle implications of gold recovery and recycling from nanowaste. *ENVIRON SCI-NANO.* 3 (5) (2016): 1133-43.
67. V. Oestreicher, C. S. García, G. J. A. A. Soler-Illia, P. C. Angelomé. Gold recycling at laboratory scale: From nanowaste to nanospheres. *CHEMSUSCHEM.* 12 (21) (2019): 4882-8.
68. K. J. Lanjekar, V. K. Rathod. Chapter 1 - microwave catalysis in organic synthesis. In: Inamuddin, Boddula R, Asiri AM, editors. *Green sustainable process for chemical and environmental engineering and science*: Elsevier; 2021. p. 1-50.
69. K. Rana, S. Rana. Microwave reactors: A brief review on its fundamental aspects and applications. *OPEN ACCESS LIBR.* 1 (2014): 1-20.
70. A. de la Hoz, Á. Díaz-Ortiz, A. Moreno. Microwaves in organic synthesis. Thermal and non-thermal microwave effects. *CHEM SOC REV.* 34 (2) (2005): 164-78.
71. K. C. Westaway, R. N. Gedye. The question of specific activation of organic reactions by microwaves. *J MICROWAVE POWER EE.* 30 (4) (1995): 219-30.
72. N. Kuhnert. Microwave-assisted reactions in organic synthesis—are there any nonthermal microwave effects? *ANGEW CHEM INT EDIT.* 41 (11) (2002): 1863-6.
73. F. Langa, P. de la Cruz, A. de la Hoz, A. Díaz-Ortiz, E. Díez-Barra. Microwave irradiation: More than just a method for accelerating reactions. *CONTEMP ORG SYNTH.* 4 (5) (1997): 373-86.
74. P. Rodríguez Seoane, N. Flórez-Fernández, E. Conde Piñeiro, H. Domínguez González. Chapter 6 - microwave-assisted water extraction. In: Domínguez González H, González Muñoz MJ, editors. *Water extraction of bioactive compounds*: Elsevier; 2017. p. 163-98.
75. D. Gupta, D. Jamwal, D. Rana, A. Katoch. 26 - microwave synthesized nanocomposites for enhancing oral bioavailability of drugs. In: Inamuddin, Asiri AM,

Mohammad A, editors. Applications of nanocomposite materials in drug delivery: Woodhead Publishing; 2018. p. 619-32.

76. C.-H. Chan, H. K. Yeoh, R. Yusoff, G. C. Ngoh. A first-principles model for plant cell rupture in microwave-assisted extraction of bioactive compounds. *J FOOD ENG.* 188 (2016): 98-107.
77. C. H. Chan, R. Yusoff, G. C. Ngoh, F. W. Kung. Microwave-assisted extractions of active ingredients from plants. *J CHROMATOGR A.* 1218 (37) (2011): 6213-25.
78. M. Llompert, M. Celeiro, T. Dagnac. Microwave-assisted extraction of pharmaceuticals, personal care products and industrial contaminants in the environment. *TrAC Trends in Analytical Chemistry.* 116 (2019): 136-50.
79. M. Mirzadeh, M. R. Arianejad, L. Khedmat. Antioxidant, antiradical, and antimicrobial activities of polysaccharides obtained by microwave-assisted extraction method: A review. *CARBOHYD POLYM.* 229 (2020): 115421.
80. V. P. Nguyen, H. Le Trung, T. H. Nguyen, D. Hoang, T. H. Tran. Advancement of microwave-assisted biosynthesis for preparing au nanoparticles using *ganoderma lucidum* extract and evaluation of their catalytic reduction of 4-nitrophenol. *ACS OMEGA.* 6 (47) (2021): 32198-207.
81. N. Arshi, F. Ahmed, S. Kumar, M. S. Anwar, J. Lu, B. H. Koo, C. G. Lee. Microwave assisted synthesis of gold nanoparticles and their antibacterial activity against *escherichia coli* (e. Coli). *CURR APPL PHYS.* 11 (1, Supplement) (2011): S360-S3.
82. S. Sunkari, B. R. Gangapuram, R. Dadigala, R. Bandi, M. Alle, V. Guttena. Microwave-irradiated green synthesis of gold nanoparticles for catalytic and anti-bacterial activity. *J ANAL SCI TECHNOL.* 8 (1) (2017): 13.
83. M. S. Rajput, N. P. Nirmal, S. J. Nirmal, C. Santivarangkna. Bio-actives from *caesalpinia sappan* l.: Recent advancements in phytochemistry and pharmacology. *S AFR J BOT.* 151 (2022): 60-74.
84. S. Warinhomhaun, B. Sritularak, D. Charnvanich. A simple high-performance liquid chromatographic method for quantitative analysis of brazilin in *caesalpinia sappan* l. Extracts. *THAI J PHARM SCI.* 42 (4) (2018): 208-13.
85. S. Badami, S. Moorkoth, S. R. Rai, E. Kannan, S. Bhojraj. Antioxidant activity of *caesalpinia sappan* heartwood. *BIOL PHARM BULL.* 26 (11) (2003): 1534-7.
86. M. A. Chowdhury, M. Choi, W. Ko, H. Lee, S. C. Kim, H. Oh, E. R. Woo, Y. C. Kim, D. S. Lee. Standardized microwave extract of sappan lignum exerts anti-inflammatory effects through inhibition of nf-kb activation via regulation of heme oxygenase-1 expression. *MOL MED REP.* 19 (3) (2019): 1809-16.
87. S. Badami, B. Geetha, S. V. Sharma, S. Rajan, B. Suresh. Microwave-assisted rapid extraction of red dye from *caesalpinia sappan* heartwood. *NAT PROD RES.* 21 (12) (2007): 1091-8.
88. R. Muangrat, W. Jirattarangsri, P. Simapisan. Response surface methodology applied to subcritical solvent extraction of brazilin compound from *caesalpinia sappan* l. Heartwood. *J APPL RES MED AROMAT PLANTS.* 31 (2022): 100408.
89. K. Wongsooksin, S. Rattanaphani, M. Tangsathit-Kulchai, V. Rattanaphani, J. Bremner. Study of an al (iii) complex with the plant dye brazilin from *caesalpinia sappan* linn. *SURANAREE J SCI TECHNOL.* 15 (2008): 159-65.
90. A. Petdum, T. Sooksimuang, N. Wanichacheva, J. Sirirak. Natural colorimetric sensor from sappanwood for turn-on selective fe²⁺ detection in aqueous media and its application in water and pharmaceutical samples. *CHEM LETT.* 48 (7) (2019): 678-81.

91. I. Aranaz, M. Mengibar, R. Harris, I. Panos, B. Miralles, N. Acosta, G. Galed, A. Heras. Functional characterization of chitin and chitosan. *CURR CHEM BIOL.* 3 (2) (2009): 203-30.
92. Q. Z. Wang, X. G. Chen, N. Liu, S. X. Wang, C. S. Liu, X. H. Meng, C. G. Liu. Protonation constants of chitosan with different molecular weight and degree of deacetylation. *CARBOHYD POLYM.* 65 (2) (2006): 194-201.
93. B.-I. Andreica, A. Anisie, I. Rosca, A.-I. Sandu, A. S. Pasca, L. M. Tartau, L. Marin. Quaternized chitosan/chitosan nanofibrous mats: An approach toward bioactive materials for tissue engineering and regenerative medicine. *CARBOHYD POLYM.* 302 (2023): 120431.
94. S. Yousefiasl, E. Sharifi, E. Salahinejad, P. Makvandi, S. Irani. Bioactive 3d-printed chitosan-based scaffolds for personalized craniofacial bone tissue engineering. *ENG REGEN.* 4 (1) (2023): 1-11.
95. V. K. Bui, D. Park, Y.-C. Lee. Chitosan combined with zno, tio₂ and ag nanoparticles for antimicrobial wound healing applications: A mini review of the research trends. *Polymers [Internet].* 2017; 9(1).
96. X. Li, F. Jiang, Y. Duan, Q. Li, Y. Qu, S. Zhao, X. Yue, C. Huang, C. Zhang, X. Pan. Chitosan electrospun nanofibers derived from *periplaneta americana* residue for promoting infected wound healing. *INT J BIOL MACROMOL.* (2022).
97. N. Bhattarai, J. Gunn, M. Zhang. Chitosan-based hydrogels for controlled, localized drug delivery. *ADV DRUG DELIVER REV.* 62 (1) (2010): 83-99.
98. F. S. Alhodieb, M. A. Barkat, H. A. Barkat, H. A. Hadi, M. I. Khan, F. Ashfaq, M. A. Rahman, M. Z. Hassan, A. A. Alanezi. Chitosan-modified nanocarriers as carriers for anticancer drug delivery: Promises and hurdles. *INT J BIOL MACROMOL.* 217 (2022): 457-69.
99. I. M. Helander, E. L. Nurmiäho-Lassila, R. Ahvenainen, J. Rhoades, S. Roller. Chitosan disrupts the barrier properties of the outer membrane of gram-negative bacteria. *INT J FOOD MICROBIOL.* 71 (2) (2001): 235-44.
100. R. Teixeira-Santos, M. Lima, L. C. Gomes, F. J. Mergulhão. Antimicrobial coatings based on chitosan to prevent implant-associated infections: A systematic review. *ISCIENCE.* 24 (12) (2021): 103480.
101. H. Zhang, Y. Zhou, C. Xu, X. Qin, Z. Guo, H. Wei, C.-Y. Yu. Mediation of synergistic chemotherapy and gene therapy via nanoparticles based on chitosan and ionic polysaccharides. *INT J BIOL MACROMOL.* 223 (2022): 290-306.
102. S. R. Bhattarai, R. B. K.C, S. Aryal, N. Bhattarai, S. Y. Kim, H. K. Yi, P. H. Hwang, H. Y. Kim. Hydrophobically modified chitosan/gold nanoparticles for DNA delivery. *J NANOPART RES.* 10 (1) (2008): 151-62.
103. S. N. Tammam, M. A. F. Khalil, E. Abdul Gawad, A. Althani, H. Zaghloul, H. M. E. Azzazy. Chitosan gold nanoparticles for detection of amplified nucleic acids isolated from sputum. *CARBOHYD POLYM.* 164 (2017): 57-63.
104. ICH Q2 (R1). Validation of analytical procedures (definitions and terminology). (2005).
105. USP43-NF38. United states pharmacopeia and the national formulary. Rockville, MD: United Book Press Inc.; 2020.
106. E. Masaenah, B. Elya, H. Setiawan, Z. Fadhillah, F. Wediasari, G. A. Nugroho, Elfahmi, T. Mozef. Antidiabetic activity and acute toxicity of combined extract of

andrographis paniculata, *syzygium cumini*, and *caesalpinia sappan*. HELIYON. 7 (12) (2021): e08561.

107. F.-K. Liu, C.-J. Ker, Y.-C. Chang, F.-H. Ko, T.-C. Chu, B.-T. Dai. Microwave heating for the preparation of nanometer gold particles. JPN J APPL PHYS. 42 (Part 1, No. 6B) (2003): 4152-8.

108. N. Dahal, S. García, J. Zhou, S. M. Humphrey. Beneficial effects of microwave-assisted heating versus conventional heating in noble metal nanoparticle synthesis. ACS Nano. 6 (11) (2012): 9433-46.

109. S. Das, A. K. Mukhopadhyay, S. Datta, D. Basu. Prospects of microwave processing: An overview. B MATER SCI. 32 (1) (2009): 1-13.

110. M. B. Gawande, S. N. Shelke, R. Zboril, R. S. Varma. Microwave-assisted chemistry: Synthetic applications for rapid assembly of nanomaterials and organics. ACCOUNT CHEM RES. 47 (4) (2014): 1338-48.

111. M. S. Latif, F. Kormin, M. K. Mustafa, I. I. Mohamad, M. Khan, S. Abbas, M. I. Ghazali, N. S. Shafie, M. F. A. Bakar, S. F. Sabran, S. F. Z. M. Fuzi. Effect of temperature on the synthesis of *centella asiatica* flavonoids extract-mediated gold nanoparticles: Uv-visible spectra analyses. AIP CONF PROC. 2016 (1) (2018): 020071.

112. M. Tran, R. DePenning, M. Turner, S. Padalkar. Effect of citrate ratio and temperature on gold nanoparticle size and morphology. MATER RES EXPRESS. 3 (10) (2016): 105027.

113. G. Muralidharan, L. Subramanian, S. K. Nallamuthu, V. Santhanam, S. Kumar. Effect of reagent addition rate and temperature on synthesis of gold nanoparticles in microemulsion route. IND ENG CHEM RES. 50 (14) (2011): 8786-91.

114. D. Wei, W. Qian. Chitosan-mediated synthesis of gold nanoparticles by uv photoactivation and their characterization. J NANOSCI NANOTECHNO. 6 (2006): 2508-14.

115. A. Pestov, A. Nazirov, E. Modin, A. Mironenko, S. Bratskaya. Mechanism of au(iii) reduction by chitosan: Comprehensive study with 13c and 1h nmr analysis of chitosan degradation products. CARBOHYD POLYM. 117 (2015): 70-7.

116. Y. Heng, D. Yuguang, Z. Junzeng. Low molecular weight and oligomeric chitosans and their bioactivities. CURR TOP MED CHEM. 9 (16) (2009): 1546-59.

117. A. Sahu, P. Goswami, U. Bora. Microwave mediated rapid synthesis of chitosan. J MATER SCI-MATER M. 20 (1) (2009): 171-5.

118. K. Ali, B. Ahmed, S. Dwivedi, Q. Saquib, A. A. Al-Khedhairy, J. Musarrat. Microwave accelerated green synthesis of stable silver nanoparticles with *eucalyptus globulus* leaf extract and their antibacterial and antibiofilm activity on clinical isolates. PLoS One. 10 (7) (2015): e0131178.

119. A. Nazirov, A. Pestov, Y. Privar, A. Ustinov, E. Modin, S. Bratskaya. One-pot green synthesis of luminescent gold nanoparticles using imidazole derivative of chitosan. CARBOHYD POLYM. 151 (2016): 649-55.

120. D. Silvestri, S. Waclawek, B. Sobel, R. Torres-Mendieta, V. Novotný, N. H. A. Nguyen, A. Ševců, V. V. T. Padil, J. Müllerová, M. Stuchlík, M. P. Papini, M. Černík, R. S. Varma. A poly(3-hydroxybutyrate)-chitosan polymer conjugate for the synthesis of safer gold nanoparticles and their applications. GREEN CHEM. 20 (21) (2018): 4975-82.

121. Y. Sameenoi, M. M. Mensack, B. M. Murphy, C. S. Henry. Competitive, non-competitive, and mixed format cleavable tag immunoassays. Methods. 56 (2) (2012): 166-73.

122. P. G. M. van Gageldonk, F. G. van Schaijk, F. R. van der Klis, G. A. M. Berbers. Development and validation of a multiplex immunoassay for the simultaneous determination of serum antibodies to bordetella pertussis, diphtheria and tetanus. *J IMMUNOL METHODS*. 335 (1) (2008): 79-89.
123. M. Zhang, J. Yang, Z. Cai, Y. Feng, Y. Wang, D. Zhang, X. Pan. Detection of engineered nanoparticles in aquatic environments: Current status and challenges in enrichment, separation, and analysis. *ENVIRON SCI-NANO*. 6 (3) (2019): 709-35.
124. A. Dedeh, A. Ciutat, M. Treguer-Delapierre, J.-P. Bourdineaud. Impact of gold nanoparticles on zebrafish exposed to a spiked sediment. *NANOTOXICOLOGY*. 9 (1) (2015): 71-80.





VITA

NAME Thana Thanayutsiri

DATE OF BIRTH 24 September 1993

PLACE OF BIRTH Lampang

INSTITUTIONS ATTENDED 2018 – Present: Doctor of Philosophy, Pharmaceutical Sciences Ph.D. Program (International program), Faculty of Pharmacy, Silpakorn University, Thailand.
2012 – 2017: Bachelor Degree, Doctor of Pharmacy (1st Class Honors), Pharmaceutical Chemistry, Faculty of Pharmacy, Silpakorn University, Thailand.

HOME ADDRESS Rama II Rd., Thakam, Bangkhuntein district, Bangkok 10150

PUBLICATION Thanayutsiri, T., Patrojanasophon, P., Opanasopit, P., Ngawhirunpat, T., Plianwong, S., & Rojanarata, T. (2020). Rapid synthesis of chitosan-capped gold nanoparticles for analytical application and facile recovery of gold from laboratory waste. CARBOHYD POLYM, 250, 116983.
Thanayutsiri, T., Patrojanasophon, P., Opanasopit, P., Ngawhirunpat, T., Laiwattanapaisal, W., & Rojanarata, T. (2023). Rapid and efficient microwave-assisted extraction of Caesalpinia sappan Linn. heartwood and subsequent synthesis of gold nanoparticles. GREEN PROCESS SYNTH, 12(1).

AWARD RECEIVED -